5-2006

Utilization of Ultrasonic Consolidation in Fabricating Satellite Decking

Joshua L. George
Utah State University

Recommended Citation

UTILIZATION OF ULTRASONIC CONSOLIDATION IN FABRICATING

SATELLITE DECKING

by

Joshua L. George

A thesis submitted in partial fulfillment
of the requirements for the degree

of

MASTER OF SCIENCE

in

Mechanical Engineering
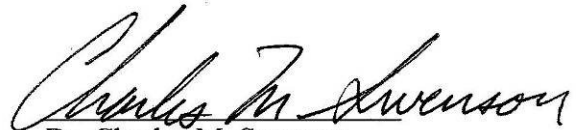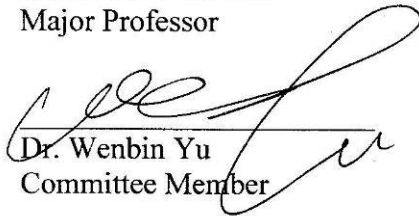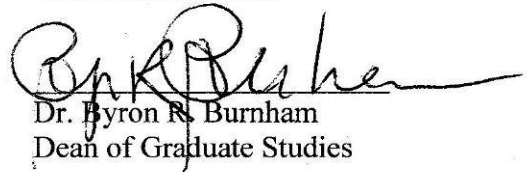

Approved:

_____
Dr. Brent E. Stucker
Major Professor

_____
Dr. Wenbin Yu
Committee Member

_____
Dr. Charles M. Swenson
Committee Member

_____
Dr. Byron R. Burnham
Dean of Graduate Studies

UTAH STATE UNIVERSITY
Logan, Utah

2006

ABSTRACT

Utilization of Ultrasonic Consolidation in Fabricating Satellite Decking

by

Joshua L. George, Master of Science

Utah State University, 2006

Major Professor: Dr. Brent E. Stucker
Department: Mechanical and Aerospace Engineering

A fundamental investigation of the use of ultrasonic consolidation (UC) to produce deck panels for small satellites was undertaken. Several fabrication methods for producing structural panels and decking were analyzed. Because of its ability to create aluminum objects in an additive fashion, and at near-room temperatures, UC was found to be a powerful solution for creating highly integrated and modular satellite panels. It also allowed a lightweight and stiff deck to be fabricated without the use of adhesives.

A series of experiments were performed to understand the issues associated with creating a sandwich-type structure using UC. The experiments used a peel test apparatus to evaluate the bond strength for various geometric configurations and materials. Aluminum 3003 was chosen as the sole material constituting the deck panel. The honeycomb lattice was found to offer the best core configuration due to its ability to resist vibration from the sonotrode and provide adequate support for pressure induced by the sonotrode. Support materials for enhancing the bonding of

the facings to the core were investigated but did not lead to implementation.

A CAD model was created to integrate the honeycomb core, facings, and modular bolt pattern into the ultrasonically consolidated structure. The model was used to develop a build procedure for fabricating the deck on the UC machine.

A finite element analysis was performed that used an equivalent properties method to represent the deck. The stiffness of a prototype deck was evaluated in a three-point bending test and the results were found to correlate with the finite element model. A sine sweep vibration test was then performed on the prototype deck panel to measure its natural frequencies.

Finally, a case study was performed on a deck built for the TOROID spacecraft. A final deck panel was designed using the results from the prototype. The deck included the USUSat bolt pattern, vented honeycomb, and a reinforced rim. The cost and benefits of the final deck panel versus traditional fabrication methods were outlined.

(100 pages)

ACKNOWLEDGMENTS

I would like to thank my major professor, Dr. Brent Stucker, for his help in the research for this thesis. He has a love for students which will be returned to him ten fold. I am greatly in debt to him for his kindness in taking an interest in my research and providing ways to complete it.

I would also like to thank the other members on my committee. Dr. Wenbin Yu has inspired me to understand the depth of a problem and to have true ethics, not only in engineering, but in all aspects of life. Dr. Swenson has played a large role in my interest in small satellites. He has been a solid pillar of knowledge and experience during my time with USUSat and CASM.

I would like to thank Joël Quincieu for inspiring me to pursue a master's degree and teaching me pride in quality craftsmanship. I also would like to thank Bonnie Ogden for her time editing this thesis.

I would also like to thank the Space Vehicles Directorate at Air Force Research Laboratory (AFRL/VS), the Air Force Office of Scientific Research (AFOSR), the American Institute of Aeronautics and Astronautics (AIAA), and the National Aeronautics and Space Administration (NASA) for sponsoring and funding the University Nanosat Program. This program had a major impact on my interest in space technology. I would like to thank the State of Utah and the Center of Excellence program for their financial support in the research. The Center for Advanced Satellite Manufacturing formed under this program will continue to invent new technologies that can have a significant impact in the small satellite community.

Finally, I want to express my appreciation to my wife, Susanna. She is everything to me and has sacrificed more than I will ever know.

Joshua L. George

CONTENTS

LIST OF TABLES

LIST OF FIGURES

LIST OF SYMBOLS

A	Area of the sonotrode's footprint
b	Panel width
c	Core thickness
D	Panel bending stiffness
d	Diameter of a hexagon
E	Modulus of elasticity
F	Bending stresses
G	Shear modulus
H	Horizontal spacing of hexagon cells
h_c	Height of the core
k	Constraint factor
L	Span length
l	length of single honeycomb cell wall
M_b	Bending moment
M_v	Shear load
N	Load
P	Critical buckling load
S	Core shear stress
T	Sandwich thickness
t	Honeycomb cell wall thickness
t_f	Thickness of facings
V	Vertical spacing of hexagon cells
ν	Poisson's Ratio
σ	Facing bending stress
σ_3	Elastic collapse stress
τ	Core shear stress

CHAPTER 1

INTRODUCTION

1.1 A New method for Satellite Fabrication

During the past few years, small satellites have emerged as a potential disruptive technology (Lewin 2004). There has been a significant push for modularity to allow smaller satellites to become as effective as many of their larger counterparts for decreased cost and with a smaller amount of time needed for design, production, and testing (Kingston 2005, Rodgers et al. 2005). This push, however, has been minimally effective, since traditional methodologies in satellite fabrication are still predominant (Panetta et al. 1998).

A similar crossroad existed in the computer world during the 1950's. The best computers still occupied entire rooms and were so costly that only a select few enjoyed their computational power. The invention of the transistor, the adoption of integrated circuit technology, and improved manufacturing techniques allowed printed circuit boards to take what was once bulky and expensive and turn them into something incredibly small and tremendously inexpensive. Due to the birth of this technology and a significant change in fabrication methodology, computers have become a useful part of every human's life.

This same type of change in accessibility and cost could have a profound impact in the small satellite world, making space more easily available to scientists, academia, and the military. Mosher and Stucker (2004) point out, however, that due to the inherent complexity and stringent requirements involved in fabricating satellites, cost remains extremely high and production times very long. Traditional methods of machining and

assembly make every satellite produced one-of-a-kind. This craftsmanship approach has been useful in the fabrication of many satellites over the past few decades but as the desire for a responsive space initiative increases, methodologies in satellite fabrication must also evolve. Advanced additive manufacturing techniques provide this desired shift in methodology where satellites are built in an automated and very repeatable process similar to the process of creating a printed circuit board. In addition, unitizing construction processes allows a satellite to be manufactured very rapidly and with significantly decreased cost (Mosher and Stucker, 2004).

One additive manufacturing technique that has tremendous potential for fabricating satellites is ultrasonic consolidation (UC). This technology uses a sonotrode (Figure 1) to apply pressure to two mating surfaces while ultrasonically vibrating one of the surfaces. In the case of aluminum, this vibration breaks up and displaces contaminants such as oxides. Without the presence of the contaminants, and with modest pressure on the two surfaces, the atomically clean surfaces join to create a true metallurgical bond without melting (White 2002). By repeating the process over and over again with aluminum tape about 0.006 inches thick, it is possible to build a three-dimensional structure from the bottom up.
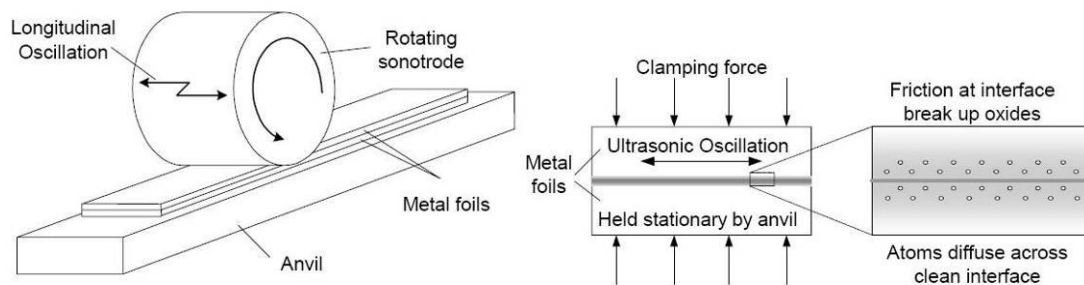
Figure 1. Schematic of UC process (Kong, Soar, and Dickens 2003).

A company by the name of Solidica has integrated the UC process into a machine (Figure 2) that also acts as a computer numerically controlled milling machine (CNC). Because features may be machined into the deposited tapes and subsequently covered with more layers, it is possible to create parts with internal features. This is very desirable since sensors, electronics, thermal regulators, and simple voids can be integrated to create a multifunctional satellite panel. In theory, it is possible, as the Center for Advanced Satellite Manufacturing at Utah State University is pursuing, to create a "printed" satellite which offers reproducibility and functionality never before seen in the satellite industry. As shown in Figure 3, a functional satellite panel can be fabricated in a series of steps where aluminum is consolidated, portions are milled away, wire tracings are deposited using the direct write process, systems are embedded, and finally solar cells are placed on the outside.

Figure 2. UC machine commercialized by Solidica.
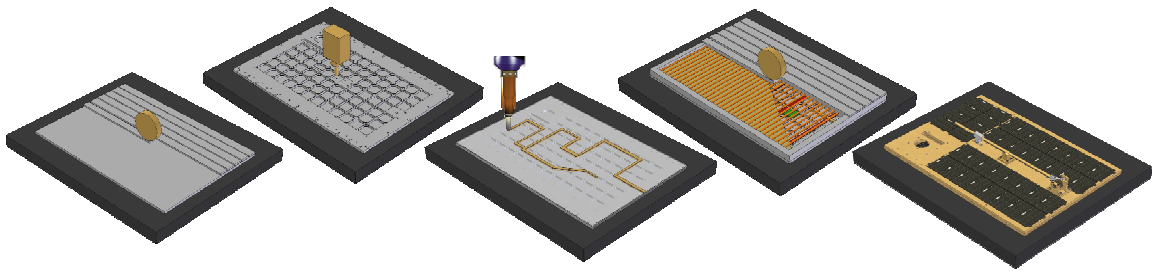
Figure 3. Advanced manufacturing techniques applied to a small satellite panel.

In an effort to support this motive and develop new small satellite technologies, this thesis employs the use of such advanced additive manufacturing techniques in the design of a structural panel for a small satellite. Research for this thesis in essence provides the bedrock for future development of this type of satellite design.

Small satellites contain several different structural panels. There are the side, top, and bottom panels which constitute the major structure of the satellite. There are also deployable panels for solar cells and deck panels which provide extra surface area to which subsystems and payload can be supported. To allow depth in the design and fabrication of a UC built panel, a small deck panel configuration is investigated.

Since the deck panel will support the payload, it is considered a primary structure. The driving requirements of this structure thus become stiffness and positional stability (Sarafin 1995). Inherent in the design of a spacecraft structure is the need to design everything as lightweight as possible. The requirements of stiffness and light weight, however, contradict each other in the solid mechanics world (Ashby 2001). Stiffness can be defined as the ratio of an applied force to the amount of deflection experienced due to the force. One is led to assume, therefore, that as a solid metal panel increases in thickness and weight, it becomes stiffer. On the other hand, as the mass increases, the

resonant frequency of a metal sheet decreases. Because the launch vehicles which put small satellites into orbit produce low frequencies with destructive capability, it is desirable to design a structure with high resonant modes. This creates the need for a tradeoff between weight and stiffness. It thus becomes the author's task to create a panel which is both light and stiff while adding the capability to become a multifunctional structure.

1.2 Thesis Layout

This thesis presents how UC can be used to fabricate satellite deck panels. A survey of the literature regarding current methods of fabricating deck panels is given in Chapter 2. This chapter also includes a survey of the research that has been performed regarding UC and its applications in rapid manufacturing. Finally, Chapter 2 will discuss methods which are used to test structural panels. Chapter 3 outlines the objectives for this research and the specific experimental tasks which have been undertaken. An experimental plan is presented to complete the objectives. The results from the experiments are presented and discussed in Chapter 4. Chapter 5 integrates the results from the experimental data into a CAD design. A structural analysis is presented in order to analyze the integrative CAD model. Chapter 6 shows the process involved for turning the CAD model into a deck panel. The structural testing of the fabricated deck panel is discussed in Chapter 7. As a final demonstration of the capabilities of UC in fabrication of a deck panel, Chapter 8 provides a case study where a deck is fabricated for the TOROID spacecraft. Finally, Chapter 9 provides conclusions and insight into future work.

CHAPTER 2

LITERATURE SURVEY

2.1 Current Methods of Fabricating Deck Panels

Over the past 40 years, many designs have arisen to solve the problem of creating structural decks and panels for spacecrafts. In order to investigate the potential solution of a deck panel being built with UC, it is important to understand the reasoning behind different panel designs.

Recent research by Dewhurst (2005) involves both analytical and numerical approaches to determining absolute minimum-weight structures. This type of structure more closely resembles those created in nature where lines of constant strain exist in the structural members. In essence, his results identify the lightest possible structure configuration for a given loading condition or stiffness requirement. Though application of his research would be desirable, his solutions are only for two dimensional structures under known static loading conditions. Because of these limitations and the absence of multifunctional capability in his work, this configuration will not be used.

Vinson (1999) has applied a methodology to create minimum-weight sandwich panels. He presents the idea that a panel contains many failure modes, any of which could cause failure of the entire panel. Different features of the panel have an associated weight which varies directly with their load carrying capabilities. When a failure occurs at any one location, any portions which have not failed are essentially "dead weight." Thus it is apparent that a minimum-weight panel is one in which all of the failure modes occur simultaneously.

Another important aspect involving structural efficiency and minimum weight is

presented by Osgood (1966). He notes that an optimum structure would weigh nothing and posses infinite strength. Because neither of these is attainable, it is necessary to define the method which will make optimization possible. In most cases, the loading condition can be well defined, thus imposing a constant strength requirement. Since the strength requirement is defined, the weight must be the variable parameter which will enable optimization.

There are two common solutions to the design problem of creating structural panels with high buckling strength relative to their weight (Larson 2003). The first solution is the use of a milled isogrid or orthogrid pattern in aluminum plate metal. The small satellite produced at Utah State University, USUSat, originally used the isogrid pattern due to its isotropic and lightweight properties (Ashby 2001). This configuration of equilateral triangles proved easy to analyze and desirable for the mission design at the time. The current USUSat design uses an orthogrid pattern (Quincieu 2003). Though the isogrid was more structurally sound and had a slightly better stiffness to mass ratio, it became cumbersome when moving components. Hence, a design change came as a result of a push for modularity.

The second solution outlined by Larson for a structural panel is a composite panel. Composites are a very appealing solution due to their incredible light weight and stiffness. They do, however, present many difficulties due to their required expertise, molds, and special equipment for manufacturing. SpaceWorks, Inc. has investigated the applications of multifunctional structures to small spacecraft (DiPalma et al. 2004). They created a composite panel with imbedded wire harnessing, as well as another structure with imbedded thermal control inserts, foils for spot shielding, and structural inserts.

The most common composite solution for deck fabrication is a honeycomb sandwich panel. This type of panel provides a large surface area and has a high ratio of stiffness to weight (Osgood 1966.) A simple form of the sandwich construction consists of two thin, stiff, strong sheets of dense material separated by a less stiff and strong central layer (Allen 1969). Generally, the central layer is much thicker to prevent shear deformation in the panel. The facings of a sandwich panel act similarly to the flanges in an I-beam. They take the bending load with one facing in compression and the other in tension. In a typical I-beam, the flanges cannot be extremely thin because of buckling on the flange tips. With sandwich panels, however, the numerous webs which compose the core support the flange tips and the thin facings will work, even to their full material yield stress (Bitzer 1997).

The structural efficiency of a honeycomb sandwich panel as compared to a solid metal sheet is illustrated by Hexcel (1999). This manufacturer has shown that a sandwich construction twice the thickness of a solid metal sheet can increase the stiffness 700 percent and the strength 350 percent, while only increasing the weight by 3 percent. A sandwich thickness of four times that of the solid metal sheet increases the stiffness 37 times and the strength 9.25 times, with only a 6 percent increase in mass.

Honeycomb is widely used in the aerospace industry. Satellites requiring large surface areas for solar cells almost always use some form of honeycomb sandwich construction. It is typically produced using one of two methods. The most common method is by expansion (Hexcel 1999). As shown in Figure 4, the expansion process connects sheets of material with adhesive lines. The resulting block is then cured and sliced to the proper dimension. A final procedure expands the sliced block into a lattice
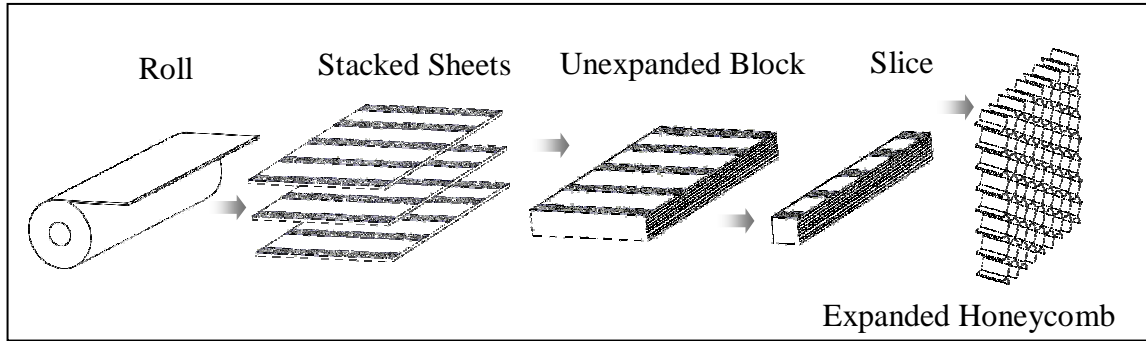
Figure 4. Conventional honeycomb production by expansion.

of connecting cells that are very thin. Later thin sheets of another material can be glued

to the core to form a sandwich panel.

Another method which is less common is used to produce higher density

honeycomb. Adhesive is applied to corrugated sheets of core material which are stacked

into blocks before curing. A final procedure cuts the corrugated block into the proper

dimensions.

Though honeycomb core can be produced in very high volumes, there are also

many drawbacks to using this type of sandwich construction. Traditional methods

require extreme precision in assembly since the process is extremely sensitive to any type

of variation. In addition, any bolted or riveted joints can cause high stress concentrations

and special potted inserts are required to prevent local failures of bolts (Shirgur and

Shannon 2000). This customization of design discourages modularity and increases both

time and cost with any slight modification in the panel.

All of the solutions mentioned above posses both good and bad attributes. This

thesis endeavors to implement the good features from each solution. First, the deck panel

adopts the sandwich honeycomb configuration of having a thick core composed of thin

webs along with rigid facings. This ensures a rigid and stiff structure. Because the

Solidica machine is used to fabricate the panel, the process does not require the

tremendous amount of expertise and precision required for honeycomb. Second, the deck

panel adopts the modular USUSat bolt pattern from the orthogrid configuration. This

helps avoid the expensive process used in potting inserts in honeycomb. Third, the deck

panel integrates the multifunctional capability of composite panels. This is possible since

features can be embedded during the build on the Solidica machine.

Figure 5 is a scale showing the various design approaches for fabricating a deck

panel. UC is proven to be a useful fabrication technique when the deck panel

configuration falls between Isogrid and Honeycomb. This is because an open isogrid

already allows any components that would have been embedded to be fastened onto the

bolt pattern. It does not need to exceed the stiffness to mass ratio of honeycomb because

the deck panel will have multifunctional features which can be much more valuable as an

end product.

2.2 Applications of Ultrasonic Consolidation

Though studies on ultrasonic welding have been performed since the late 1950's

(Daniels 1965, Weare, Antonevich, and Monroe 1959), it has not become a useful metal

additive manufacturing technique until the new millennium. Even still, the transition of
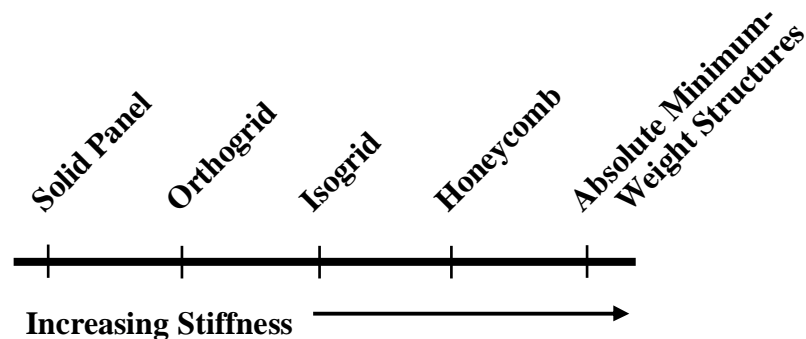
Figure 5. Scale to quantify usefulness of new fabrication technique.

UC from research to industrial applications remains in its infancy. For the last few years, Kong, Soar, and Dickens (2003) have been performing experiments to determine the optimum process parameters, weld strength, characterization, and plastic deformation of various aluminum alloys. They have also been investigating the use of the UC process for the production of monolithic aluminum components and continuously fiber-reinforced metal matrix composites. They obtained results by preparing specimens which could be tested in bend tests, lap-shear tests, peel tests, and micro structural examinations. The output of each experiment was evaluated both theoretically and experimentally. They have concluded that a continued exploration of the process will result in a low cost, solid-state fabrication process for aerospace technologies.

Additional research is taking place in other areas of UC. Matsuoka (1998) has found a way to weld various ceramics to metals at room temperature. Studies have also been performed at Kanagawa University in Japan regarding ultrasonic butt welding of aluminum and stainless steel plate specimens (Tsujino et al. 2002).

UC emerged as a direct metal manufacturing technique and rapid prototyping technology in the late 1990's. Research by Johnson (1998) at Tufts University found that UC can be used to make prototypes similar to other rapid prototyping machines with the added benefits of low energy consumption, modest space, and no emission of fumes. In addition, he found that ultrasonic metal welding had many advantages over other rapid prototyping methods due to the fact that bonds could be formed between dissimilar metals which could allow prototypes of sandwiched materials to be produced. He also noted that since there is no melting, dimensional accuracy is highly achievable. Finally,

he noted the fact that off the shelf materials can be used which offers a low-cost solution to rapid prototyping.

Johnson's work involved the integration of a simple ultrasonic metal welder and a high-speed cutter to make very simple three dimensional dog bones for testing. His work was followed by Gao (1999) who analyzed the mechanics of ultrasonic metal welding during rapid prototyping. He used analytical modeling, finite element analysis, and experimental data acquisition to look at static and dynamic effects in the elastic and plastic flow regions during welding.

Solidica has performed extensive research to generate process windows for creating metal tooling and parts. Their work represents the integration of UC and CNC milling capabilities to additively fabricate an aluminum part. The literature does not show any current applications of UC for fabricating a satellite structure.

The UC machine manufactured by Solidica uses four parameters when performing UC to achieve a bond. These include the weld pressure, weld speed, substrate temperature, and amplitude of oscillation from the sonotrode. Research regarding the optimum process parameters has been performed by Kong. His intention has been to "subject the specimens to a series of tests that would explore the mechanical and physical properties of the welds produced for any given combination of process variables" (Kong, Soar, and Dickens 2003). Kong's work did not include the influence of temperature; however, a more comprehensive set of tests including temperature was recently performed by Janaki Ram et al. (2006).

Solidica's patented UC process is capable of bonding different materials together. This is possible because many materials are susceptible to the inter-laminar metallurgical

bonding induced by ultrasonic excitation. The research for this thesis, however, limited its use of materials to alloys of aluminum. This limitation was imposed to keep the focus on the structural design of a satellite deck panel. Furthermore, aluminum is one of the most common types of sandwich-panel materials used in space structures (Triplett 1995).

Two alloys of aluminum have had research performed regarding their capability in a UC application. The first alloy was aluminum 3003. This alloy was extensively tested and used by Solidica. Additionally, Kong, Soar, and Dickens (2004) performed useful research on the optimum process parameters for ultrasonically consolidating this alloy. The second alloy that has been investigated is aluminum 6061. Characterization of this alloy in the UC process was also investigated by Kong, Soar, and Dickens (2003). Both alloys contained many properties favored by NASA concerning stress corrosion and resistance to crack propagation (NASA 1992).

One of the critical design aspects of a honeycomb-type panel is the achievable height to width ratio. UC, however, has historically not produced excellent results with ribs that were tall and thin. Limitations of freestanding ribs were investigated by Robinson et al. (2006) for ribs parallel to the tape direction, perpendicular to the tape direction, and at a 45 degree angle.

In their work, Robinson et al. (2006) laid aluminum tapes and machined each layer to get three different widths of ribs (Figure 6). Each of the three widths was tested parallel to the tape direction or longitudinal, perpendicular to the tape direction or lateral, and with a 45-degree rotation.
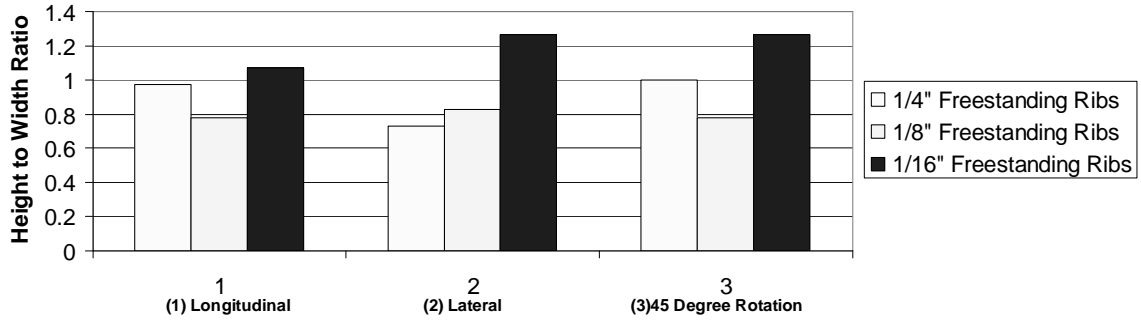
Figure 6. Height to width ratios for freestanding ribs (Robinson 2006).

The ribs were carefully observed until consolidation failed to take place with newly added layers. From the results in Figure 6, it is evident that problems occur once the freestanding rib height exceeds the dimensions of its width.

Due to the nature of how UC is implemented, there are limitations on build configurations. One of the most important considerations is the mechanical differential vibration between the substrate and newly deposited layer, or "scrubbing" action, which generates the metallurgic bond. It is absolutely imperative that the scrubbing action of the sonotrode be performed on a stationary platform to which the aluminum tape can be consolidated. As the z height of the part increases, a cantilever effect allows the part to vibrate (Figure 7). This impedes the scrubbing action necessary to break up oxides on the surface of the tape and can create a very poor bond between aluminum layers. Parts that accommodate a large surface area and have a small z height are stiff and therefore the problem does not exist. For conventional sandwich panels, however, thin webs are the key to a lightweight structure, which presents problems in the fabrication process.

Traversing
direction of
sonotrode

Oscillation from sonotrode

Bulky Part
remains
stationary

Thin Part
vibrates due to
cantilever effect
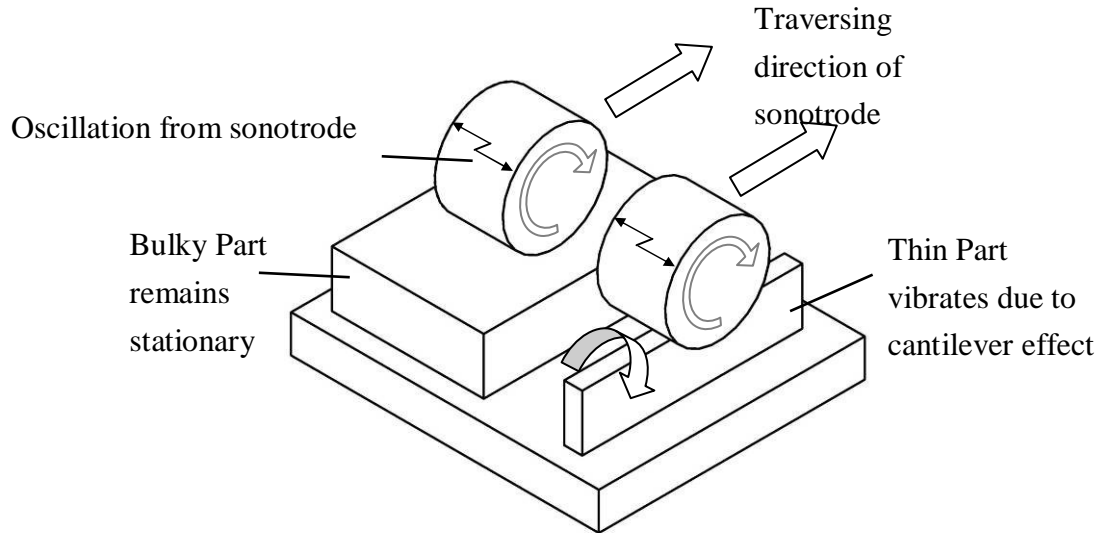
Figure 7. Effects of different height to width ratios.

In addition to thin webs for a core, it is more advantageous to use a thick core or taller webs. This is due to the effect of the core thickness, c, on the bending stiffness, D, of a sandwich panel (ASTM C 393-00):

$$D = \frac{E \cdot \left(T^{3} - c^{3}\right) \cdot b}{12} \tag{1}$$

If the modulus of elasticity, E, the width of the panel, b, and the sandwich thickness, T, are all held constant, the stiffness increases rapidly with increasing core thickness.

Additionally, the core shear stress, τ, and the facing bending stress, σ, can be defined as in ASTM C 393-00 by:

$$\tau = \frac{N}{(T+c) \cdot b} \qquad (2)$$

$$\sigma = \frac{N \cdot L}{2 \cdot t_f (T+c) \cdot b} \qquad (3)$$

where N is the load placed upon the midpoint of the sandwich panel, and t_f is the facing thickness. If c is allowed to increase independent of the other variables, the stresses experienced in the panel decrease. It is therefore evident that a thicker core or web structure is stiffer and capable of withstanding more stress.

One additional form of research that can be very useful in an aerospace application is the use of a support material during the build. This could be used to support thin webs during consolidation to provide the stability required to get a good bond. Many additive manufacturing processes, such as Selective Laser Sintering (Chua, Malkus, and Plesha 2003), use a support material to support such features during the build process. Later, the support material can be removed.

Solidica has performed research using a Tin-Bismuth alloy as a support material. Though they had success with this alloy, it is not ideal for a satellite deck panel. The panel will be flown in space where materials will exist in a vacuum. Tin has a tendency to grow "whiskers," or crystal fibers, in such an environment. These fibers can bridge a pair of metal contacts and destroy a satellite's electrical system. For this reason, support materials for space applications other than tin-bismuth, such as a polymer, are necessary.

2.3 Testing of Structural Panels

There are two basic segments of testing that must occur in the development of a sandwich panel. The first segment involves testing to understand the quality of bonding between the core and the facings.

Normally, honeycomb specimens undergo compressive testing and plate shear testing (Bitzer 1997). These test help in measuring the compression modulus as well as the honeycomb shear strengths and moduli. Their applicability to UC built specimens, however, may be minimal since the core is not produced by gluing thin pieces of aluminum together.

Another series of test such as the flatwise tension test and climbing drum peel test are usually performed on the assembled sandwich panel to test the effectiveness of the bond between the honeycomb core and the thin facings. The flatwise edge test pulls the facings in tension to separate them from the core. The climbing drum peel test peels off a facing by rolling it around a drum. The failure modes in both tests are revealed as core tearing, cohesive failure of the adhesive, or failure of the adhesion to the honeycomb or facing. Both of these tests are excellent ways of evaluating the integrity of a honeycomb sandwich panel (Bitzer 1997).

Kong (2005) found that a standard test method used for measuring the resistance of adhesives to peeling was an effective method for determining weld quality for specimens built with UC. From his research, he found that as the number and size of contact points within the welded interface increased, so did the average resistance to peeling. Though the peel test results were not as smooth as those for adhesives, they still revealed a general trend in weld effectiveness. This test, in effect, is very similar to the

climbing drum peel test. Not only does it work better with parts made using UC, it also has been performed previously and therefore has data with which to compare.

The second segment of testing involves testing the assembled sandwich panel for a macroscopic view of its stiffness, strength, and resonant modes. This enables a verification of the structural requirements imposed by the payload.

A commercial honeycomb manufacturer, Hexcel (1999), has indicated that the beam-flexure test is often used to evaluate overall sandwich panel performance. This test, often called the 3-point bend test, is particularly important since it verifies how the core and facings work together to give the overall properties of the panel. The test can be performed with a single or double point load. The stiffness of the panel can be calculated using the imposed force and deflection at the mid span of the panel (Bitzer 1997). The ASTM standard: Standard Test Method for Flexural Properties of Sandwich Constructions (ASTM 2004) can be used to determine the properties of flat sandwich constructions subjected to flatwise flexure. Such an experiment can be carried out in a quasi-static manner with a very low loading speed (Paik, Thayamballi, and Kim 1999).

Another aspect of testing involves vibration testing. Osgood (1966) points out that the principal types of loading on a spacecraft are the vibratory and static accelerations imposed by the launch vehicle. This type of testing is of particular importance since very little vibration testing has been performed on parts made by UC.

CHAPTER 3

EXPERIMENTAL RESEARCH PLAN

3.1 Experimental Objectives

The objective of this thesis was to demonstrate the capability of the UC process for fabrication of a deck panel. Though the theoretical capability of a direct metal manufacturing technique in fabricating a multifunctional satellite was apparent, it was important to focus on the issues associated with a build in the real world. Thus a series of experiments were performed to originate the design of the deck panel's geometry and the effects of different build parameters on the assembly. The following list outlines the specific experiments undertaken to acquire such information.

- Developed a method for implementing peel tests

- Determined a benchmark peel strength based on established UC optimum parameters

- Determined the best material for the experiments for this thesis

- Evaluated the effects of rib direction on bond strength

- Evaluated the effects of core lattice shape on bond strength

- Determined the effects of varying core lattice size on bond strength

- Investigated the importance of heating the baseplate on bond strength

- Investigated the effect of amplitude on the bond strength

- Investigated the effect of welding speed on bond strength

- Investigated the effect of polymer support materials on bond strength

3.2 Experimental Approach

The most important features of the panel were strength and stiffness, which depended on the macroscopic behavior of the consolidated product. Thus in assembling a sandwich panel, the most critical feature was the effective bond between the core and the facings. Following testing similar to Kong (2003), experiments were performed to evaluate the quality of the bond between a specific core geometry and a facing.

3.2.1 A Method for Implementing Peel Tests

The Standard Test Method for Floating Roller Peel Resistance of Adhesives (ASTM D3167-03a) was used to create a fixture for specimens created on the Solidica machine. There were some deviations in the dimensions of the specified test fixture to accommodate the larger plates used in the Solidica machine. Also, the speed was changed from 152 mm/min to 52 mm/min to allow comparison with Kong's data. The higher separation rate was originally intended for adhesives which have smoother peeling. Slowing the separation rate down allowed a more controlled environment to account for discrete bonding. As shown in Figure 8, the apparatus accepted a rigid plate with an aluminum tape attached to one of its surfaces. The unbonded portion of the tape was fed around a roller and clamped to a stationary surface. A Tinius Olsen tensile testing machine was then used to lift the entire peel test fixture. As the whole apparatus was elevated, a load cell was used to measure the force to remove the consolidated tape from the rigid plate. Two additional rollers were used to keep the rigid plate from tipping forward or backward. Once the midpoint of the rigid plate was directly over the clamp, the peel test was terminated and the process repeated for the other end of the rigid plate. Figure 9 shows the peel test fixture integrated in the tensile test machine.

Peel Test Fixture

Rigid Plate

Clamp

Aluminum Tape
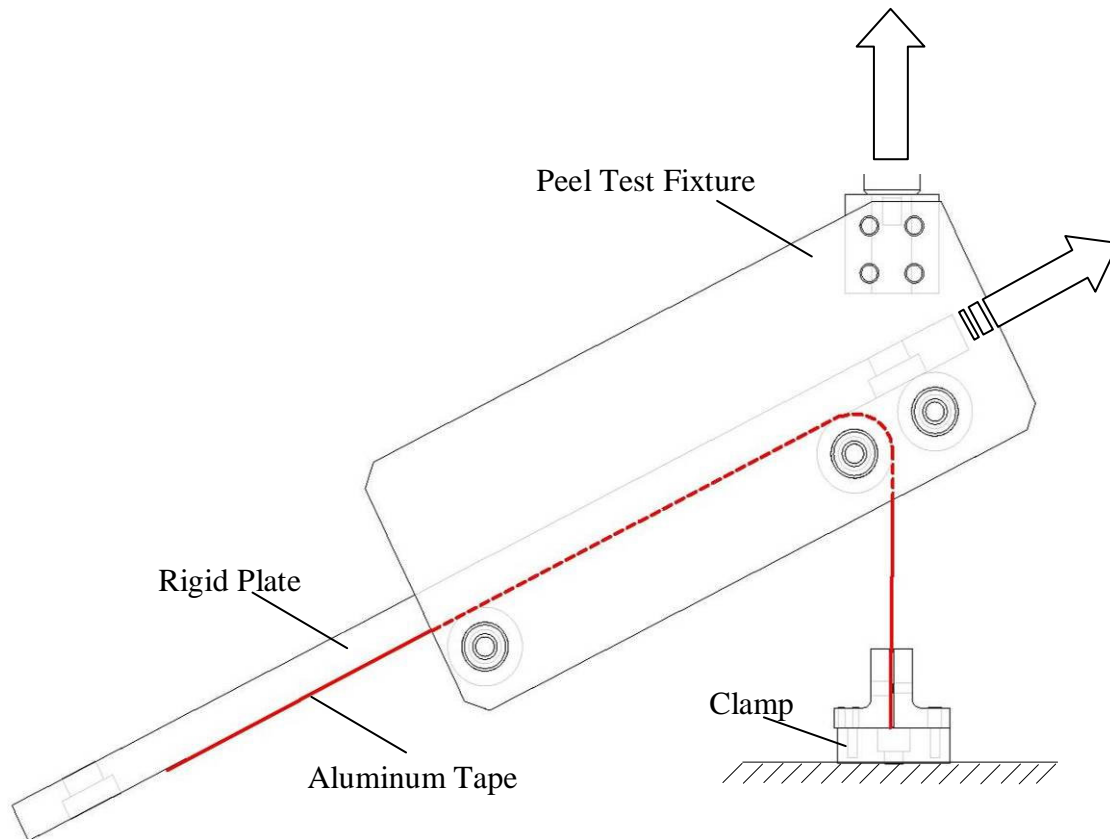
Figure 8. Apparatus for performing peel tests on consolidated specimens.

The load cell used in the peel tests was a 100 pounds force (lbf) capacity load cell

manufactured by Interface Force Measurements Ltd. The load cell possessed a

nonlinearity error of ±0.05%, hysteresis of ±0.03%, and nonrepeatability of ±0.02%.

Using an output voltage of 3mV/V, an excitation of 15VDC, and a 10^{-4} accuracy

display, the resolution of the load cell was calculated to be 0.22 lbf.

In order to perform the weld effectiveness experiments in the peel test apparatus,

it was first necessary to determine how consistent results from experiment to experiment

could be obtained. To allow for a fixture that could fit in the peel test setup, a plate size

of 4 x 14 inches was chosen. Six specimens were consolidated to an aluminum plate in

the exact same manner to investigate the standard deviation (Figure 10).

Figure 9. Loaded peel test apparatus with 4 inch plate and three consolidated tapes.

Per recommendation from the manufacturer of the UC machine, the temperature was held constant at 300 degrees Fahrenheit during the consolidation. The tapes were then peeled off of the plate and the force restraining the peeling was measured as a function of displacement.

The location of the consolidated tape on the platform was also investigated for its effect on data consistency. It was noted in the preceding experiment that test results differed considerably depending on the locating of the test specimen on the plate. To understand this effect, three tapes were consolidated parallel to the long direction of the rigid plate. The peel strengths for the three locations were then measured in a test.
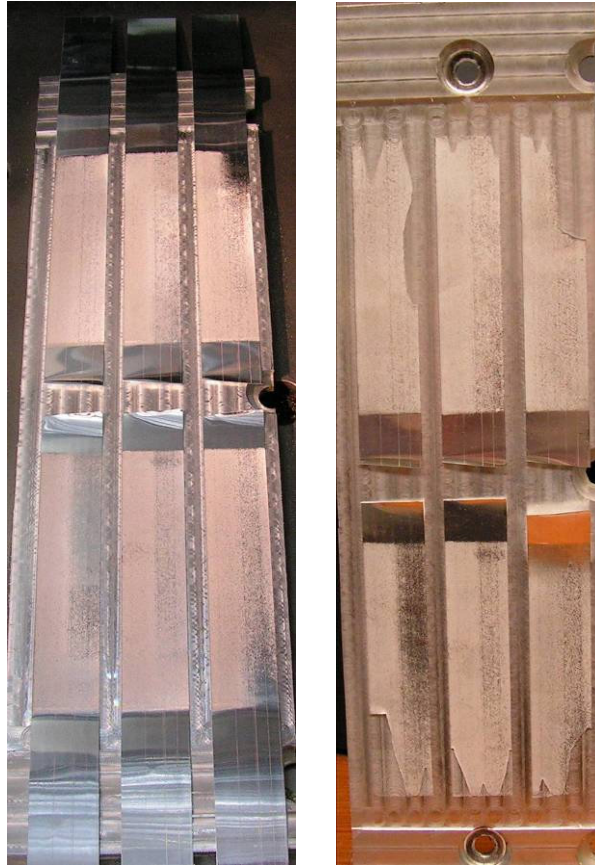
Figure 10. Consolidated tapes before and after peel tests.

The last experiment needed for developing a method for implementing the peel

test involved the heat plate which was a heated platen that maintained an aluminum

baseplate at a constant temperature and also provides mounting points for stabilization. It

had a slight crown on its surface such that when a baseplate was bolted down, it was flush

against the heat plate. This crown, however, caused a problem when using the small 4 x

14 inch plates. Edge effects from the crown caused a slight gap between the plate and the

heat plate along the plate edges. This gap allowed vibration of the plate which prevented

good consolidation. It was speculated that even the larger 14-by-14 inch plates

experience some degree of edge effect.

Before a tape was consolidated to a baseplate, the plate was milled to provide a

flat, clean surface. An experiment was created which investigated the difference in milling the baseplate with x-direction passes versus y-direction passes. After milling a certain direction, a tape was consolidated to the plate and a peel test was used to determine the average strength of the bond.

These three experiments were used to prove that a four-inch plate could be used to implement peel testing with consolidated aluminum. The results from the experiments would provide the extent of data consistency, the best location for the specimens, and the best orientation to mill the baseplate.

Finally, to be able to compare peel tests to one another, it would be necessary to establish a benchmark peel strength based on the UC optimum parameters from Janaki Ram's (2006) work. This would be accomplished by consolidating a tape using the optimum parameters: temperature = 300° Fahrenheit, amplitude = 16μm, feedrate = 66 ipm, force = 1750 N. The tapes would be consolidated over a solid baseplate to give the greatest strength of bond. After performing this several times, an upper limit on the bond strength could be established. This bond strength, representing a full tape width, could then be used to evaluate the quality of a bond over an area of less than a full tape width. This would also provide a method to validate the bond between the facing and the core.

3.2.2 Material Selection

An experiment was designed to test the effect of using a plate made out of aluminum 6061 with the T6 temper as opposed to the 3003 alloy with the H18 temper. This involved simply consolidating a tape to each of the different plates. Similar parameters were used in both cases.

3.2.3 Rib Direction

As was discussed in the literature survey, conventional sandwich panel is most useful when the core is composed of thin, tall webs. This presents a unique challenge for the UC process since a thin, tall web cannot provide the rigidity for scrubbing the oxide layer. One way to mitigate the vibration effect is to orient the ribs such that the mechanical oscillation of the sonotrode is applied to the stiffest direction of the ribs. The sonotrode oscillates perpendicular to the direction it travels when laying tapes. Thus ribs which lie perpendicular to the traversing direction of the sonotrode would allow the best bond to be created. This does present some problems, however, since the sonotrode dips into channels between ribs if there are no other structural members, due to an applied force which is given to the sonotrode. A 45-degree angle on the ribs relative to the traversing direction, however, gives the sonotrode enough cross section to avoid dipping and still provides stability against vibration.

To evaluate this effect of rib direction on bonding strength, an experiment was performed where ribs were milled (Figure 11) parallel, perpendicular, and at 45 degrees with respect to the traversing direction of the sonotrode. A single tape was consolidated to each of the rib specimens and was removed in the peel test.

It must be noted, however, that the results of this experiment only apply to ribs without the support of a lattice type structure. The following section will investigate the need for a properly designed lattice for the sandwich panel core. Though lattice cores would be used in the deck, the lattice segments would still act as ribs with respect to the oscillation of the sonotrode. This would be of particular importance when orienting the segments of the core with respect to the traversing direction of the sonotrode.
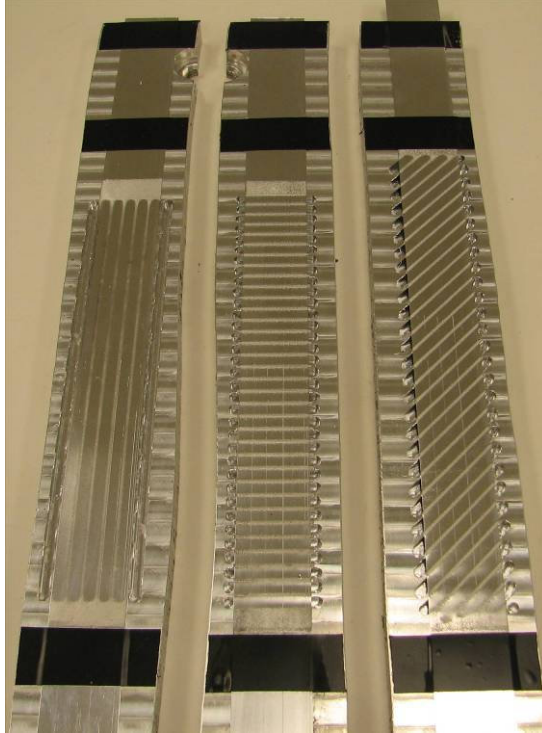
Figure 11. Test specimens for determining the effect of rib direction on peel strength.

3.2.4 Core Lattice Shape

The solution to creating a core resides not in using single ribs to support the facings but rather to use connecting ribs to form cell walls which form a core lattice. The connecting cells in a sandwich panel can have a variety of geometric configurations. The most common is the hexagonal shape which resembles the honeycomb made by bees. This configuration is the most commonly used core due to its rigid and lightweight design. Other designs include triangles, waves, and squares. Because the Solidica machine lays tapes by applying pressure and traversing in one direction, there are special considerations for the core composition.

Out of all of the possible core configurations, only hexagons and triangles provided support for the sonotrode while providing ribs in the stiffest direction. By argument it was difficult to determine if the hexagon was a better core lattice than the

triangle so an experiment was created to compare how the two different geometries interacted with the oscillation of the sonotrode. To compare the two geometries directly, the dimensions of the triangle were chosen such that both the triangle and the hexagon enclosed the same area of 0.25 inches. Then 0.040 inch thick ribs were created for both geometries. As before, the specimens were created by milling the patterns into a 0.5-inch thick aluminum plate to a depth of 0.11 inches. A skin consisting of one tape was applied to each specimen as shown in Figure 12. The tapes were then removed in a peel test.

3.2.5 Core Lattice Size

It was desirable to evaluate the effect of core lattice size on bond strength. The larger hexagon tested in the previous experiment was chosen because it is the largest hexagon which allows the sonotrode to always straddle two lines of ribs for support. The thickness of the honeycomb ribs was chosen based on visual clues that smaller ribs could not support the pressure of the sonotrode during consolidation. It was desirable, however to investigate how using thinner honeycomb ribs with smaller honeycomb areas would affect the bond.
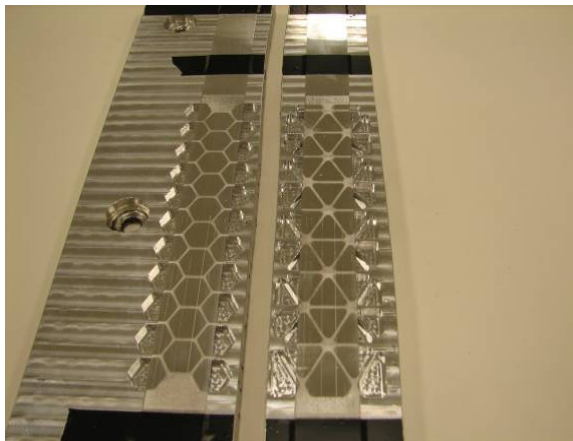
Figure 12. Test specimens for comparison of bonding for hexagons and triangles.

The hexagons in Figure 12 had a circumscribed diameter of 0.62 inches with a rib thickness of 0.04 inches. It was compared to a milled hexagon with a circumscribed diameter of 0.40 inches and rib thickness 0.02 inches. The two different configurations were milled into a baseplate and an aluminum tape was consolidated to the top surface as shown in Figure 13. The tapes were then removed in a peel test.

3.2.6 Heating the Baseplate

The Solidica machine is equipped with a heater plate because it is understood that elevated temperatures enhance UC to give a better bond. To understand the significance of heating the plate, the peel test was used to remove a tape that had been consolidated at 70 degrees Fahrenheit and a tape that had been consolidated at 300 degrees Fahrenheit.
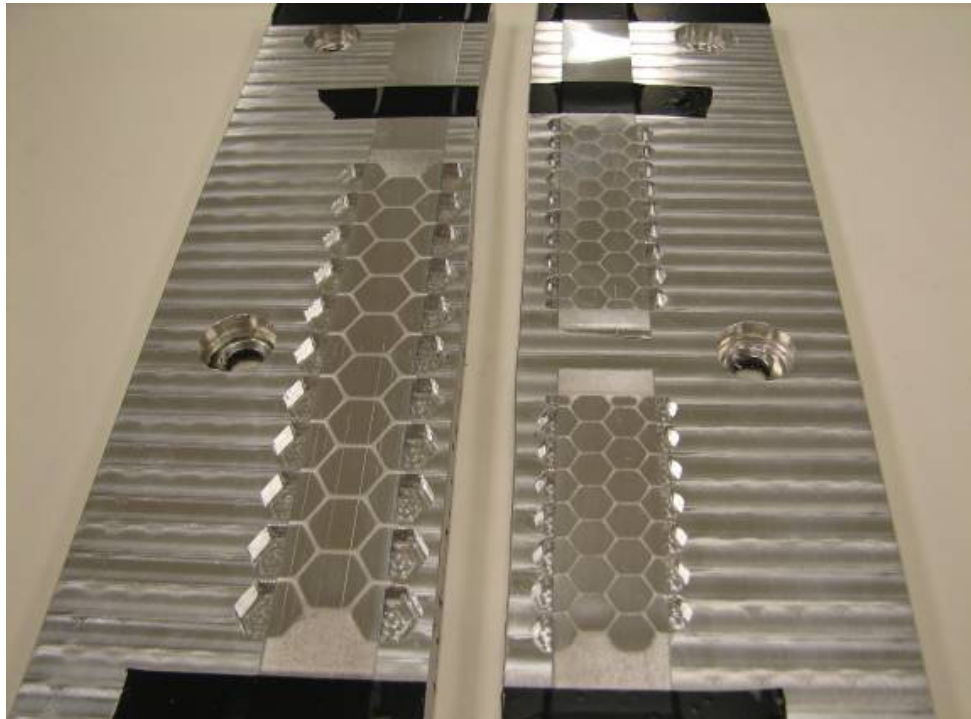
Figure 13. Test specimens for testing effect of honeycomb size on peel strength.

3.2.7 Welding Amplitude

Though Kong (2003) had conducted a series of tests that would explore the mechanical and physical properties of the welds produced for any given combination of process variables, and research on the process parameters has taken place at Utah State University (Janaki Ram, 2006), it was important to explore optimized parameters for tall ribs connected in a hexagonal pattern. The network of interlocking beams has been found to behave vastly different to the input parameters than the typical solid builds produced on the machine. This included the weld pressure, weld speed, and amplitude of oscillation from the sonotrode. It was observed that the bond strength was significantly better when the amplitude was increase from 16 microns to about 19 microns.

In order to understand the effects of increasing the amplitude, an experiment was designed to contrast the peeling strength of a honeycomb core bonded with a sonotrode amplitude of 16 microns and one bonded with 18 microns of amplitude.

3.2.8 Welding Speed

The welding speed was also tested to understand its impact on the bond strength. On a hexagonal core, a tape was consolidated at 100 percent and 80 percent of 30 in/min. The tapes were removed in a peel test.

3.2.9 Support Materials

There were a series of experiments performed to investigate the utility and feasibility of using a polymer as a support material. In the first experiments, a thermoplastic was used based on its ease of removal with acetone. After the material was used to fill empty portions between milled ribs, the surface was cleaned with a flat pass

milling operation (Figure 14) and a tape was laid on the substrate containing ribs reinforced with the polymer.

Another experiment was performed to test if a thermoset would give better results since it would be less prone to smearing. A hexagonal lattice was milled into a plate of aluminum as shown in Figure 15. The top portion was left without support material to allow comparison of the ribs with and without the material. The lower portion was filled with a thermoset. The thermoset was much harder than the thermoplastic, especially at the build temperature of 300 degrees. Again, a tape was consolidated to the surface of the substrate.
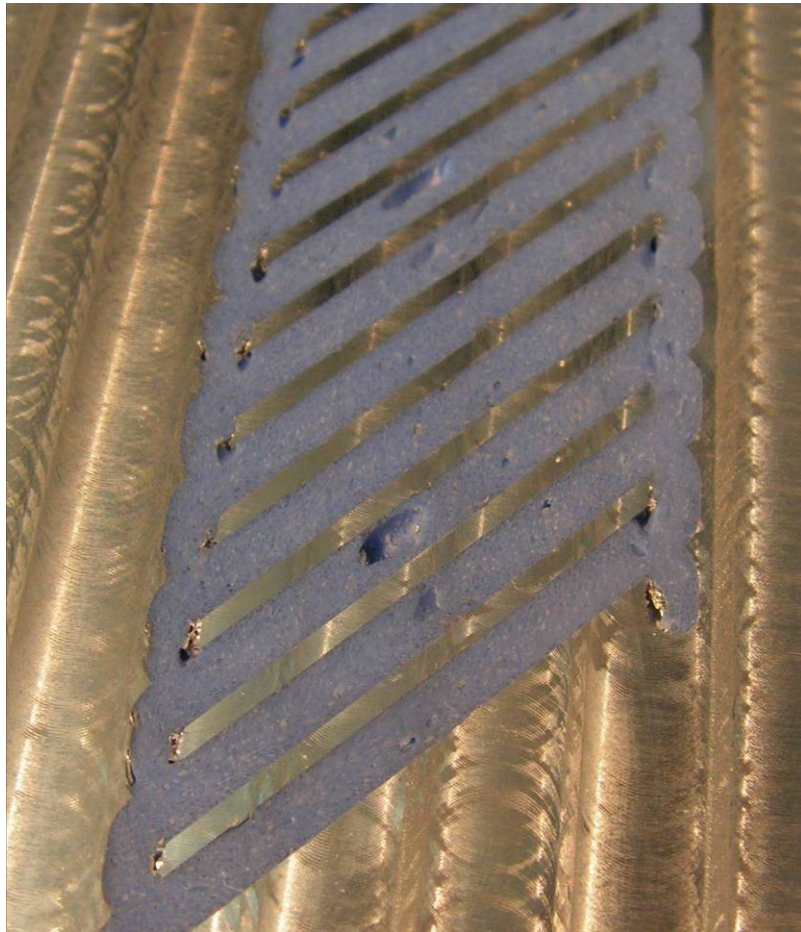
Figure 14. Test specimen for thermopolymer support material.

Figure 15. Test specimen for thermoset support material, with honeycomb lattice.

A final experiment was designed to eliminate the possibility of contaminating the top surface of the ribs with any polymer. Ribs were milled out of an aluminum plate and a thermoset polymer was applied to the pockets in between the ribs. Then there was a second machining operation to remove a few thousandths of the support material. Finally, there was a flat pass milling operation to clean the surface of the protruding ribs as shown in Figure 16. This order of operations verified that the surface was clean and that the protruding ribs were supported with a stiff material. The height to width ratio of the protruding ribs was maintained in the workable range of less than 1. A tape was consolidated to the substrate as before.

Figure 16. Test specimen for contamination-free support material experiment.

CHAPTER 4

EXPERIMENTAL RESULTS

4.1 Development of a Method for Implementing Peel Tests

Generally, there were three reactions to the peel test based on the strength of the bond. The weakest bonds would allow a smooth peel where the resistance to peeling could be observed over the length of the experiment without any tearing. Specimens with extremely good bonding would tear the aluminum tape from the rigid plate before peeling would occur. This can be seen in Figure 17. Note the serrated appearance of the torn interface. This type of tear results from the fact that there is an ever varying gradient of weld effectiveness. When failing, the tear would propagate through the weakest bonded areas. On the plots for such peel tests, there would usually be a sharp incline, a short peak, and then an extremely rapid fall to zero.
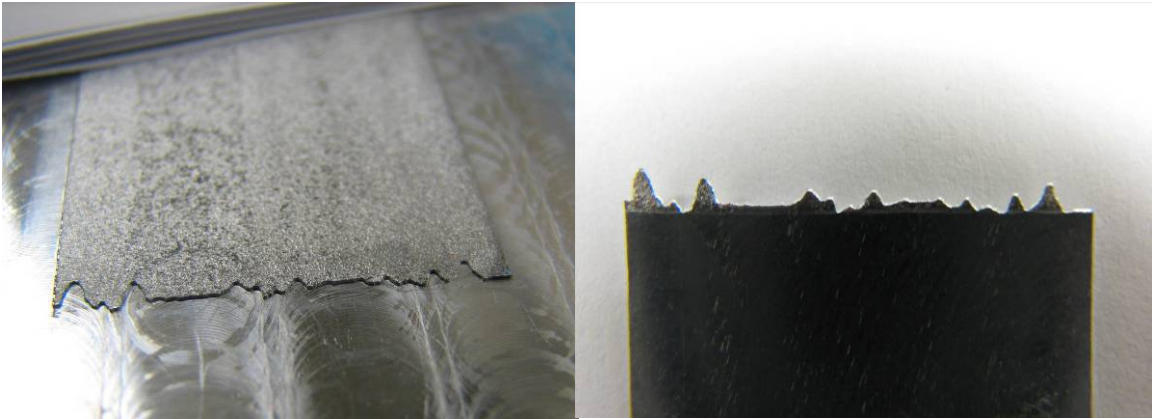
Figure 17. Failed specimen after being consolidated to a baseplate and peeled in a peel test.

The third reaction to the peel test was where a small portion of the tape would tear due to a greater variation in weld effectiveness over the tape. In the load versus extension plots for this type of reaction, the load would increase to a peak and then slowly slope down to zero. This is because the tear would decrease the effective cross section being tested. Thus all data after the peak were invalid for comparison with other results. This type of reaction was seen in Figure 10.

As was shown in the right side of Figure 10, the tapes were peeled in the peel test apparatus and the results for the rightmost tape are found in Figure 18. This was done to show the consistency of the results from the peel test. The results show a maximum load of about 20 lbf before the tapes would begin to tear. Kong (2005) obtained an average of about 20 lbf during his peel tests with the 3003 aluminum alloy. Similar parameters were used in both cases, however Kong did not use a heated baseplate to enhance his bonding. This will be further discussed toward the end of the experimental results chapter.
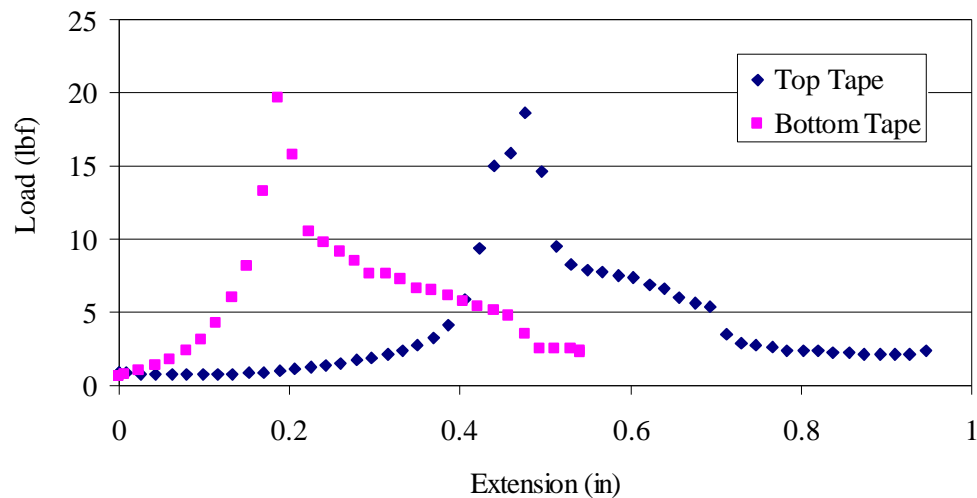
Figure 18. Peel test results for 3003 aluminum (300° F, 16 μm, 28 ipm, 1750 N).

Note that the top and bottom specimens have a similar trend that is offset. The offsetting is due to the fact that one tape was set up with more slack in the apparatus. The results for the center and leftmost tapes had a similar pattern. The difference in maximum load experienced during the peel test for the different specimens revealed the approximate standard deviation. The values obtained for the leftmost and rightmost tapes for two separate occasions were used to calculate the standard deviation. The center tape values were omitted because they were typically much greater due to stability of the baseplate. This will be discussed in the following paragraphs. From the data, a standard deviation of 4.32 lbf was computed.

From the results (Figure 19) of the peel test for tape location on the 4 inch plate it is evident that the center tape was achieving a much better bond than the left and right tapes. After multiple tests, it was also evident that the center tape gave more consistent results from experiment to experiment. It was decided that for specimens on the small 4-
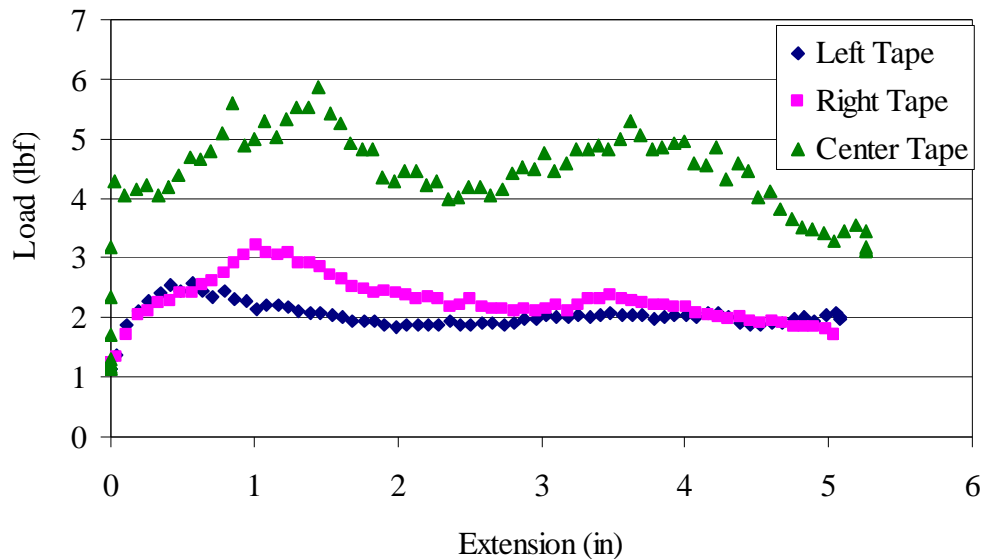
Figure 19. Peel test result for 6061 aluminum for tape location (70° F, 16 μm, 28 ipm, 1750 N).

by-14-inch plates, only one tape at the center of the plate would be used for experimentation.

The experiment which investigated the difference in milling the baseplate with x-direction passes versus y-direction passes produced the data found Figure 20. The results showed numerically equal trends, but the y-direction plate clear showed substantially less scatter. This is because of the direction of the machining lines made by the CNC. Though these features were typically smaller than 0.0001 inches, they did have an effect on the data scatter. Since the x-direction plate clear was perpendicular to the direction of tape lay, the machine lines presented more bumps for the consolidated tape. The higher areas were welded better and showed up in the peel test with regions of high and then low bond strength. Making these machine lines run parallel with the tape virtually eliminated the oscillating spike effect and smoothed out the data. For this reason, only y-direction plate clears were used for the experiments using the 4 in plate.
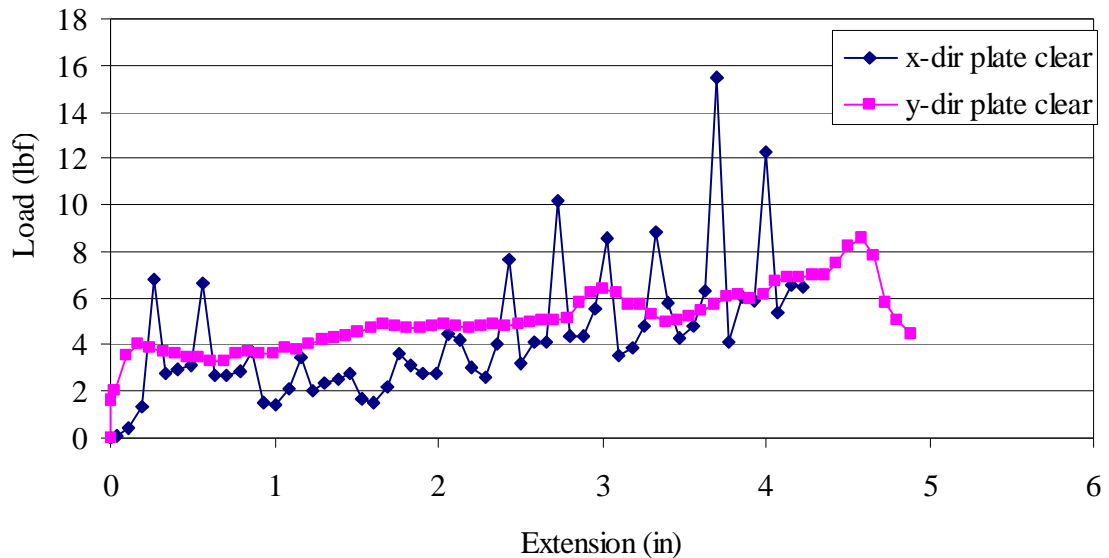
Figure 20. Peel test data for plate clear orientation (70° F, 16 μm, 28 ipm, 1750 N).

Figure 21 shows the results from peeling a tape which was consolidated at the optimum parameters and over a solid baseplate. The results from two trials show that the maximum obtainable bond strength for these parameters is about 43 lbf. All of the following UC experiments will be compared with the benchmark value followed by a discussion of any reasons for deviation.

4.2 Material Selection

The results from peeling a tape off of plates made of 3003-H18 aluminum and 6061-T6 Aluminum are shown in Figure 22. From the plot it is evident that there is a much better bond if the plate is made of the 3003 alloy. The data for the 3003 alloy was scattered and quickly dropped after a maximum point because of tearing in the tape. The 6061 data was more consistent because the bond was not very effective. Thought it was desirable to investigate the possibility of using the 6061 alloy in the deck panel due to its greater strength for ultimate, yield, shear, and fatigue, it presented many problems due to
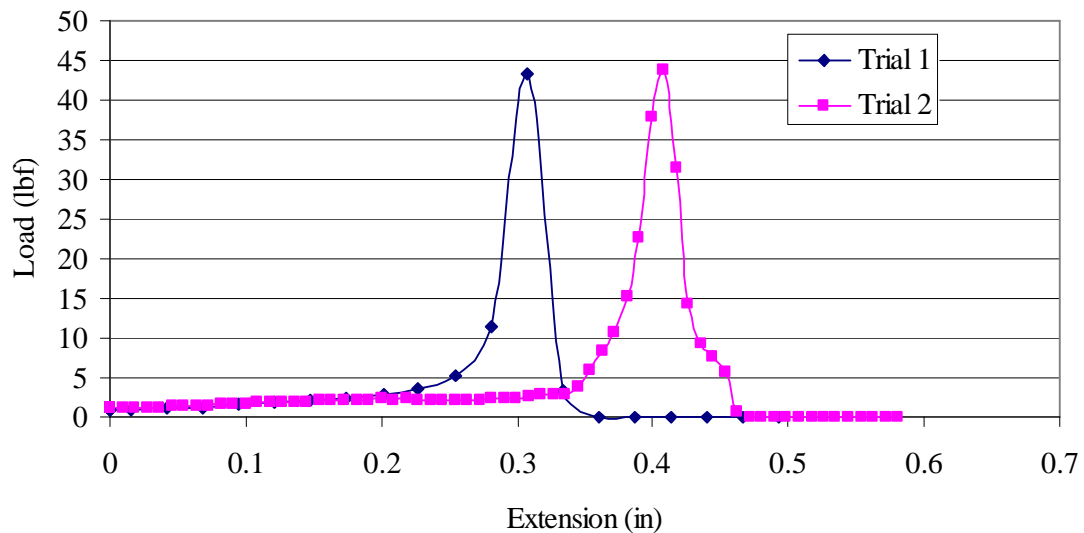
Figure 21. Peel test data for maximum bond strength (300° F, 16 μm, 28 ipm, 1750 N).
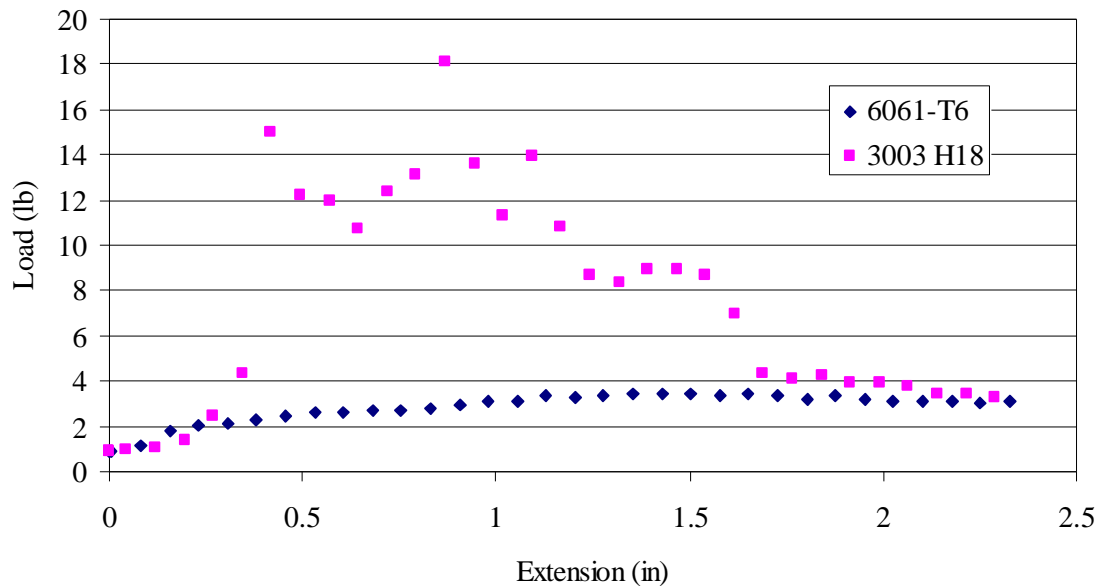
Figure 22. Comparison of resistance to peeling for two types of aluminum baseplates (70° F, 16 μm, 28 ipm, 1750 N).

its characteristic of rapidly forming a strong oxide. For this reason, 3003 was used for the experiments and development of the deck panel for this thesis.

In this experiment, the UC parameters (temperature = 70° F, amplitude = 16μm, feedrate = 28 ipm, force = 1750 N) were chosen to give a weaker bond than that obtained using the optimum parameters. Peel test of samples consolidated using the optimum parameters often provided limited data since the tape would tear after a short distance. Since some of the experiments in this section required a sample over the entire welded region, a weaker bond prevented tearing during the peel test and suitable data was obtained.
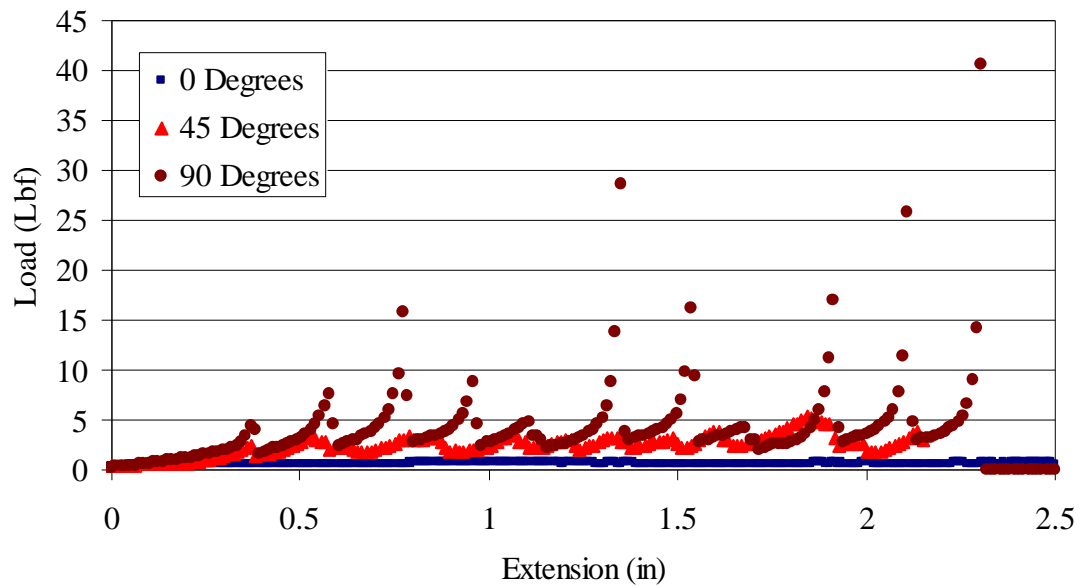
Figure 23. Peel test results for variation in rib direction (300° F, 18 μm, 30 ipm, 1750 N).

4.3 Rib Direction

The results from the peel test which looked at rib direction are found in Figure 23. The ribs parallel to the traversing direction of the sonotrode would not bond and the graph reflects only the weight of the plate being tested. The 45-degree ribs provided a weak bond. As had been theorized, the ribs perpendicular to the traversing direction provided a substantially better bond with a peak load of about 40 lbf before failing. The failed tape exhibited very small serrated teeth, indicating an extremely uniform and dense bond. The data shows many peaks which indicate where the tape was bonded to a rib.

This data is comparable to the benchmark data of 43 lbf since similar properties were used. The amplitude was increased slightly to aid in bonding for ribs. This will be discussed later. The spike of 41 lbf shows a facing can be bonded to a rib just as well as the solid baseplate used in the benchmark experiment.

The results of the preceding experiment narrowed the options of practical core

configurations to include a series of lines perpendicular to the traversing direction of the sonotrode, squares, hexagons, and triangles. The series of perpendicular lines, however would not have worked due to the fact that the core would have provided rigidity in only one direction. A lattice of squares would have provided rigidity in both directions but would have presented problems in fabrication. The first layer for the facing would have bonded to the perpendicular parts of the square lattice but not to the segments parallel to the traversing direction of the sonotrode. There could have been a rotation of the panel during the build to allow tapes to be laid in a cross hatching manner but the second layer of tapes would still have not bonded due to the fact that the first layer was unable to bond to some sections. This left hexagons and triangles as potential core configurations.
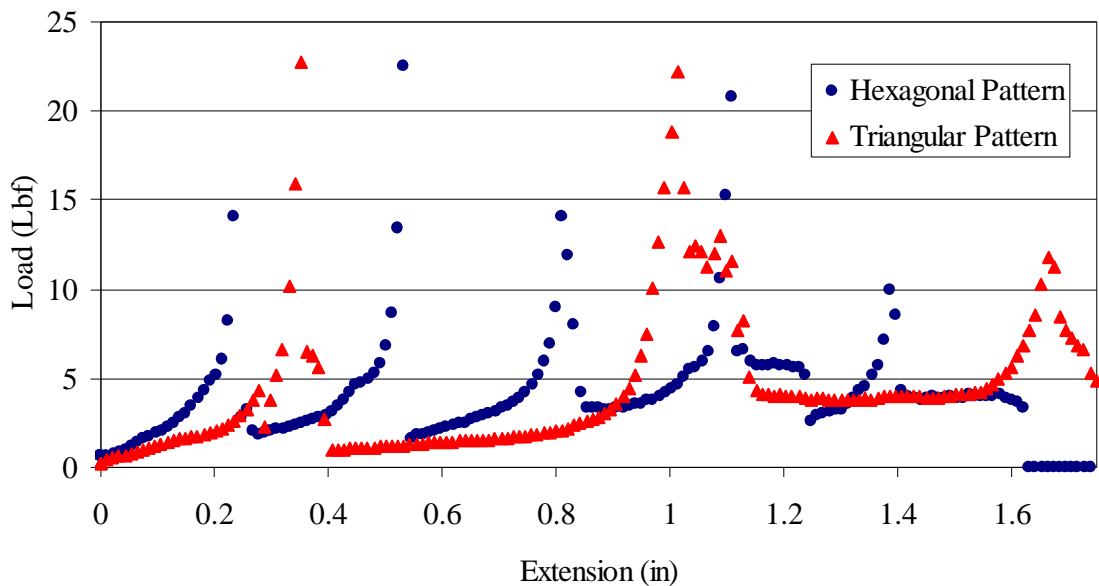
Figure 24. Peel test results for hexagonal vs. triangular pattern (300° F, 18 μm, 30 ipm, 1750 N).

4.4 Core Lattice Shape

Results (Figure 24) from the peel test to investigate the effects of core lattice shape showed that the effective bond had a maximum value of 23 pounds for both the hexagonal and triangular lattices. In the case of the hexagon, the peak load occurred at the location of maximum bond width. In the benchmark tests, this was the width of a tape which was 0.94 inches.

The hexagon, however, had a maximum bond width of only 0.41 inches. Because this area was only 43.6 percent of the area of a full tape, the equivalent bond strength of the hexagon was 52 lbf. This far exceeded the value obtained in the benchmark test and showed that very good bonding can occur between segments of honeycomb and a facing. Because of the fact that hexagonal structures use the least amount of material to create a lattice of cells within a given volume, hexagons were chosen to be the shape for the core. The hexagons were oriented such that no cell walls were parallel with the traversing direction of the sonotrode.

4.5 Core Lattice Size

The results of the peel test for determining the effects of hexagon size on bond strength are found in Figure 25. From the results, it is evident that decreasing the size of the hexagon and the rib thickness has minimal impact on the peel strength. Because the larger hexagons allow the creation of a lighter core for a given amount of volume, it was chosen to be the best configuration for the deck panel.

The data is comparable to benchmark tests and shows equivalent bond strength of 41 lbf. This again demonstrates that very good bonding is taking place between segments of the honeycomb and the facing.
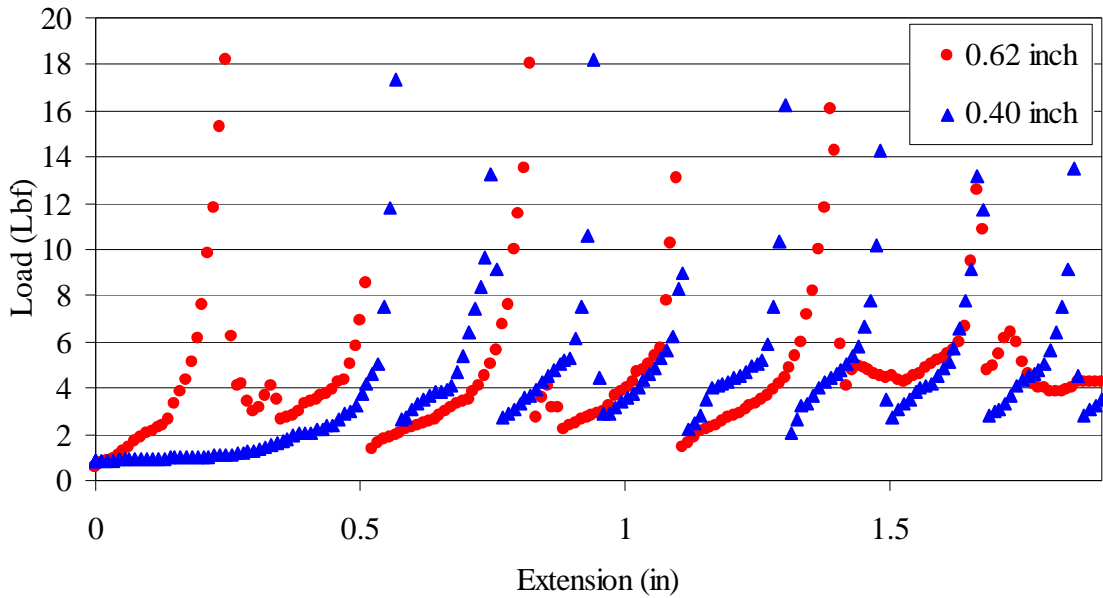
Figure 25. Results for variation in hexagon size (300° F, 18 μm, 30 ipm, 1750 N).

4.6 Heating the Baseplate

The results to heating the baseplate during consolidation are found in Figure 26. The 300 degree specimen shows a spike of 44 lbf at 0.4 inches of extension. This data correlates with the maximum bond strength found in the benchmark test. The 80 degree specimen has more of a consistent peel resistance but at a significantly lower value. It is interesting to note that the room temperature peak of 16 lbf corresponds somewhat to the average value obtained by Kong (2005) during his peel tests. From the results of the experiment, it is evident that heating to 300 degrees Fahrenheit can create a bond with nearly three times the peel strength. For this reason, the deck panel would be built at 300 degrees Fahrenheit.
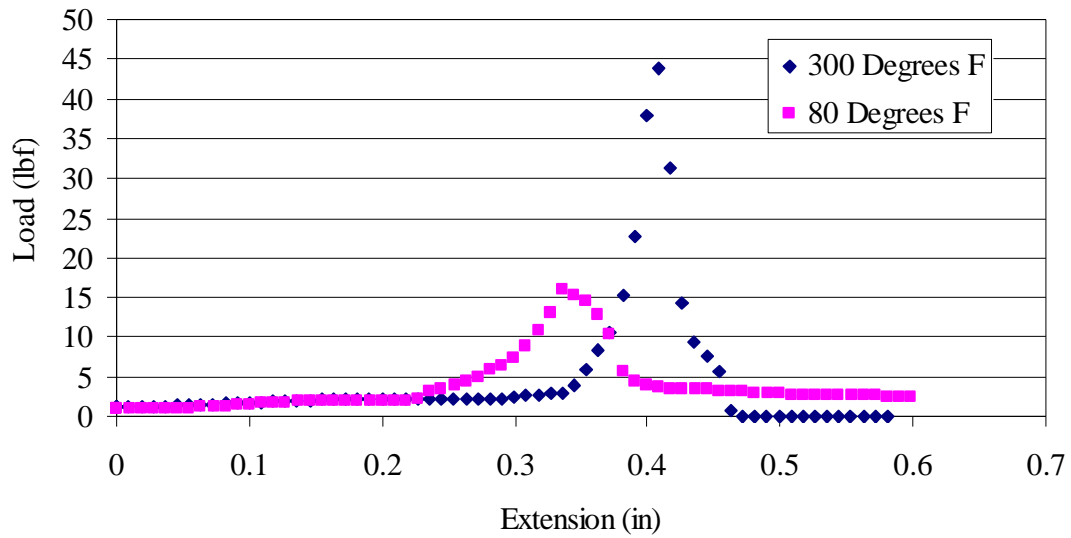
Figure 26. Peel test data for heat effect (16 μm, 66 ipm, 1750 N).

4.7 Welding Amplitude

The results to the amplitude test are shown in Figure 27. From the results, is evident that increasing the amplitude of oscillation of the sonotrode to 18 microns creates a better bond. The optimum parameters for UC bonding had been determined for full tape width samples. It was noted that this amplitude did not generate very good bonds with thin walled structures. The amplitude was increased to 19 microns for another specimen and it appeared that the large amount of energy going into the welding process caused slight tearing of the tapes due to excessive oscillation. Thus 18 microns was used for the fabrication of the deck panel. This data correlates with the average values found in the benchmark tests.
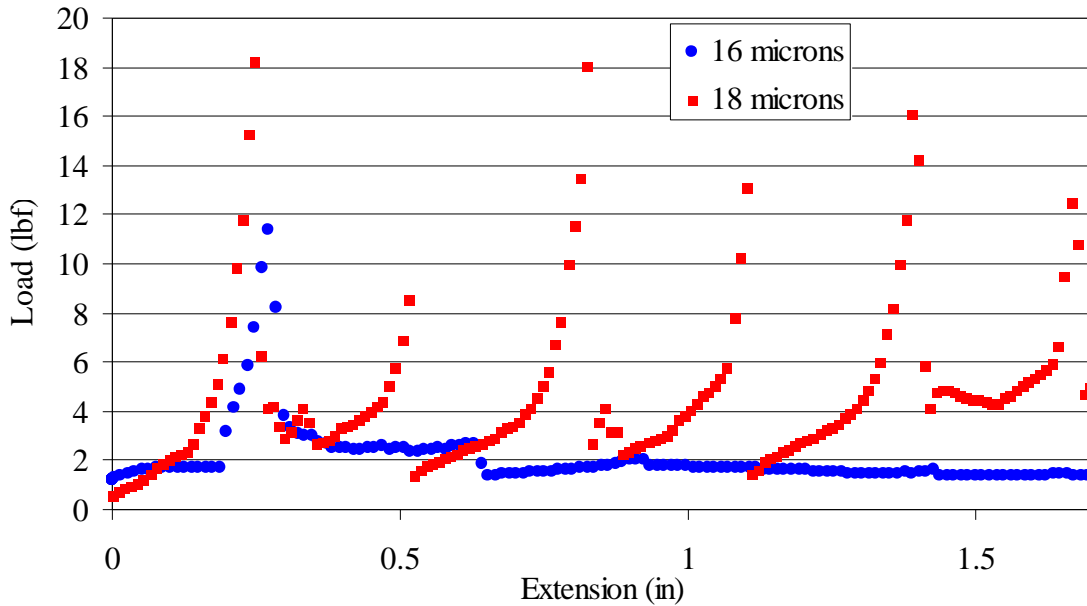
Figure 27. Peel test results for variation in amplitude (300° F, 30 ipm, 1750 N).

4.8 Welding Speed

The results to the experiment on welding speed for 24 ipm and 30 ipm are found in Figure 28. This peel test shows that decreasing the speed of the sontrode's travel can adversely affect the bond. This is most likely due to overworking the surface such that bonds are formed and subsequently broken. The 100 percent trial correlates with the average values found in the benchmark tests.

4.9 Support Materials

It was extremely difficult to make the tape stick to the ribs when using a thermoplastic support material, likely due to smearing of the polymer over the metal surface. During the one instance where the face sheet did stick, however, the bond was incredibly strong. Though it was not possible to perform a peel test, a photo (Figure 29) was obtained showing a peeled tape with and without the thermoplastic support material.
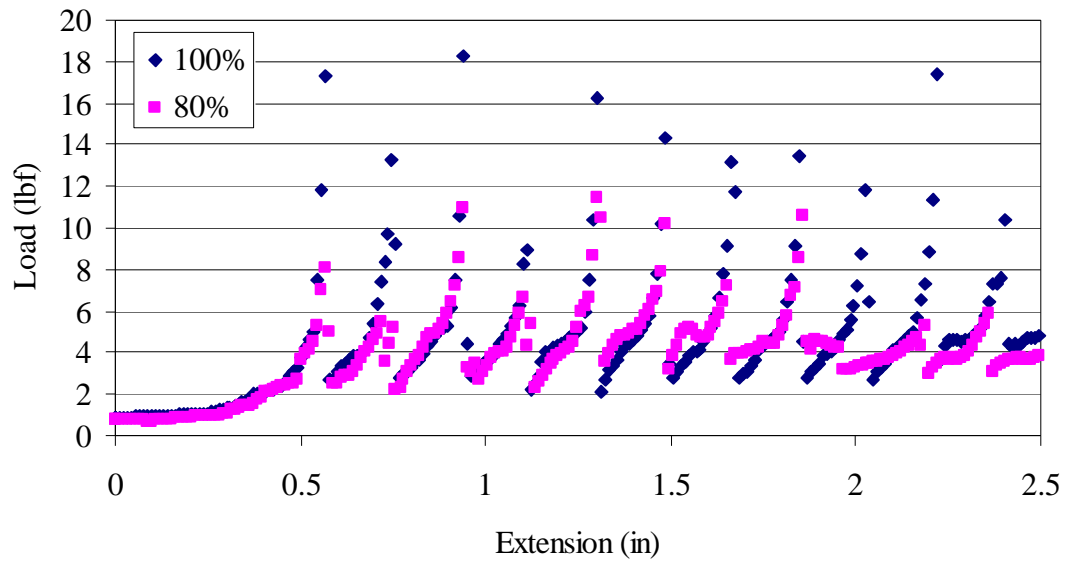
Figure 28. Peel test results for variation in welding speed (300° F, 18 μm, 1750 N).

The left side of the image in Figure 29 shows 45-degree lines, which indicates that the sonotrode had applied pressure and scrubbed the tape against the ribs. The lines were clean because the removal was easy and smooth. The right side of the image shows a distorted tape that was consolidated to the supported rib structure. Upon close inspection, one can see that excellent bonding occurred between the rib and the plate.
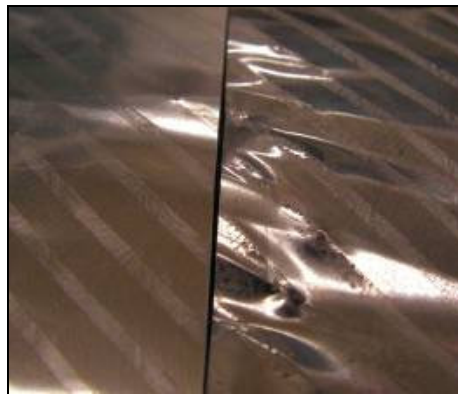
Figure 29. Peeled tape showing 45-degree lines.

This is evidenced by ripples along the 45-degree lines which were caused by the tape sticking to the ribs during removal.

It was theorized that the thermoplastic was either too soft and thus allowing the ribs to vibrate, or that it was smearing on the surface of the ribs. The smeared polymer would significantly impact and perhaps totally disallow any bonding to occur between the ribs and the aluminum tape.

The results from the thermoset experiment were similar where bonding did not occur. The final support material experiment involved verifying the surface was clean, however, the same results were obtained. Due to the projected development time needed to create a sufficient support material, research on support materials was abandoned and ongoing research efforts were directed elsewhere.

CHAPTER 5

INTEGRATIVE CAD MODEL AND STRUCTURAL ANALYSIS

The integrative CAD model integrates the configuration results from the peel tests to create a functional deck panel for a small satellite. It also integrates solid mechanics theory into the geometry of the panel to give the best compromise between what is ideal and what is realistic for fabrication in the UC machine. Once the integrative model is defined, it provides something which can be analyzed by finite element analysis.

5.1 CAD Model

From geometry, the vertical and horizontal spacing of the cells were found to be:

$$V = \frac{\sqrt{3}}{2}d + t \tag{4}$$

$$H = \frac{3}{4}d + \sqrt{t^2 - (\frac{t}{2})^2} \tag{5}$$

where d is the diameter of the hexagon, and t is the thickness of the honeycomb walls. These formulas were input into a CAD model in Solid Edge and a honeycomb lattice was created. To create a bolt pattern, it was necessary to leave several of the hexagons filled so they could later be tapped and used as fastening points.

The overall dimensions of the deck panel were based on the maximum size that could be currently accommodated in the UC machine. The deck panel was chosen to be 10.75 inches by 10.75 inches. It was also decided to include a reinforced rim around the

perimeter of the deck to give support to the core and allow reinforced sections to be used

to mount the deck to brackets which would attach to the satellite side panels. Holes were

selected to be through holes for these mounting points. The finalized design, without the

top facing, can be found in Figure 30.

Solid mechanics theory shows that two facings can be separated by a lightweight

core to increase the moment of inertia of the panel without any significant increase in

weight. Thus as the core increases in thickness, the panel's stiffness-to-weight ratio

dramatically increases. Though the width to height ratio of a rib plays an important role

in fabricating a free standing rib, it has little impact on a lattice of connecting cells. The

thickness of the panel, therefore, is based on the maximum allowable thickness for the

volume allotted and the maximum depth the Solidica machine can mill. For the first

prototype deck, a thickness of 0.36 inches was chosen.
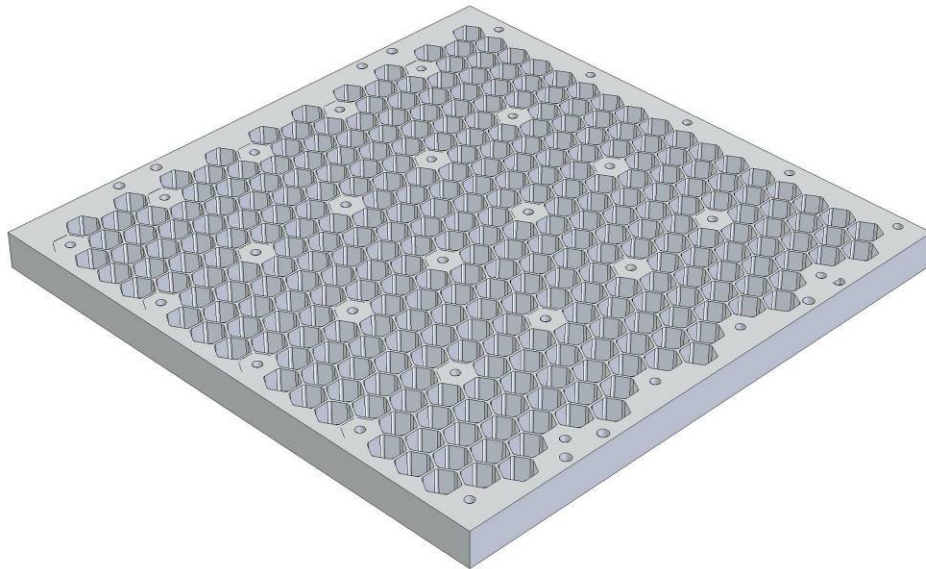
Figure 30. Integrative CAD model without the top facing.

The design approach to the panel did not follow the typical design approach found in the aerospace industry. Typically, structural elements are designed to support a given loading profile. After a safety factor is applied, any extra mass is eliminated. USUSat has the idea of creating a modular platform that is capable of multiple missions. Though there is a slight mass penalty, the added benefits of modularity and flexibility greatly outweigh such factors. The deck panel was designed such that the deck was composed of the lightest form that could be fabricated on the UC machine and the largest size that could fit in a small satellite bus based on the USUSat design. After the panel was fabricated, testing and finite element modeling was used to verify that the design satisfied the structural requirements imposed by the satellite mission. If there happened to be a discrepancy, the design of the deck panel could be modified to compensate for the discrepancy.

Some other geometric factors that must be determined are the size of the honeycomb cells and the thickness of the cell walls. Though the ideal core would posses very thin walls, the geometries in this panel are limited based on the amount of load imposed by the Solidica machine during consolidation. It is important to avoid exceeding the critical buckling load of the lattice determined by the second moment of inertia of the walls of the cells, which is defined by Gibson and Ashby (1988) as:

$$P = \frac{KE}{(1-\nu^2)} \frac{t^3}{l} \qquad (6)$$

where k is a constraint factor, E is the modulus of elasticity, ν is Poisson's ratio, t is the wall thickness and l is the length of a single cell wall. Because the Solidica machine

operates at a specified load during consolidation, and since K, E, and v are constants which depend on the geometry chosen, t can be solved as a function of l. The length of a single cell wall ultimately determines the size of the cells, which is limited by the need to have the sonotrode always straddling at least two cell walls. As was discussed earlier, this provides the sonotrode a flat surface to which a tape can be consolidated. A cell wall size of 0.31 provides a sufficient lattice while maximizing the area of empty region.

The critical buckling load formula above can now be used to determine the thickness of the cell walls since the formula relates cell wall thickness and cell wall length. The formula is more useful when expressed as the elastic collapse stress. The parameter K can be approximated to be 4 based on the fact that the honeycomb cell is neither completely free nor rigidly clamped. For regular hexagons and v = 0.3, the formula becomes:

$$\frac{\sigma_3}{E} = 5.2\left(\frac{t}{l}\right)^3 \tag{7}$$

The elastic collapse stress can be rewritten as the force applied by the sonotrode divided by the area which is acted upon. The sonotrode has a contact area of 0.197 x 0.94 inches. This area, however, acts only on the honeycomb rib line enclosed by the area. For the cell wall length of 0.31 inches this area can be calculated using:

$$A = lt + \frac{2t(0.197 - t)}{\sin(60)} \tag{8}$$

Plugging in 10,000 psi for E, 1750 Newtons for the force, and 0.31 for the cell wall length gives a minimum cell wall thickness of 0.024 inches. To allow for some margin of safety, and due to success in experiments, a cell wall thickness of 0.040 inches is suitable for the honeycomb lattice.

Finally, the dimensions of the facings were determined. The standard thickness used in regular honeycomb of 0.025 inches corresponded well with the thickness of four consolidated layers and was therefore used. During builds where facings were consolidated to honeycomb cores, it was noted that the first couple of layers contained minor defects due to the sharp interface between the facing and the core when applied at high amplitudes. The third and fourth layers, however, contained negligible defects and therefore provided the minimum facing thickness for a well built sandwich panel.

5.2 Analysis Technique

Cook, Malkus, and Plesha (1989) have noted that in modeling, the analyst seeks to exclude superfluous detail but include all essential features, so that analysis of the model is not unnecessarily complicated yet provides results that describe the actual problem with sufficient accuracy. Bitzer (1997) said of sandwich panels that programs have already been written using finite element analysis but it can be a very expensive and time consuming experience. This is further supported by Grediac (1993) who stated that, "modeling a whole honeycomb for a finite element analysis cannot reasonably be considered because of the complexity of such a structure." Though computers now allow more sophisticated calculations in less time, honeycomb still remains incredibly complex when modeled with exact geometry. The model often times has too many degrees of freedom to be studied with usual finite element programs. Because the emphasis of this

thesis existed in the design of the panel using UC and not so much in the correlation between experimental and theoretical results, and because substantial literature has been published on the analysis of honeycomb core, this thesis implemented an approximation technique for the structural analysis.

The simplest analysis technique for a sandwich panel has been commonly called the "effective" or "equivalent" properties method. This method uses the geometry of the facings and core lattice to create a solid plate or skin which approximates the properties of the real sandwich panel. The approximations, however, do present some error based on the fact that the equations drop terms, since some features of sandwich panels do not contribute significantly to the stiffness. In essence, the equations attempt to negate the negligible terms and emphasize terms which provide the greatest values.

The equivalent single skin plate method outlined by Paik, Thayamballi, and Kim (1999) considers the rigidity of panels, with equal facing skin thickness, separately for in-plane tension, bending, and shear. Paik solves the equations to obtain the equivalent thickness, t_{eq}, the modulus of elasticity, E_{eq}, and the shear modulus, G_{eq}.

$$t_{eq} = \sqrt{3h_c^2 + 6h_c t_f + 4t_f^2} \tag{9}$$

$$E_{eq} = \frac{2t_f E}{t_{eq}} \tag{10}$$

$$G_{eq} = \frac{2t_f G}{t_{eq}} \tag{11}$$

In the equations above, h_c is the height of the core, t_f is the thickness of the

facing, E is the modulus of elasticity of the facing and G is the shear modulus of the

facing. From the geometry of the prototype deck panel,

$$h_c = 0.285 \, \text{in} \tag{12}$$

$$t_f = 0.024 \, \text{in} \tag{13}$$

$$E = 10000 \times 10^3 \, \text{psi} \tag{14}$$

$$G = 3630 \times 10^3 \, \text{psi} \tag{15}$$

From the equations above, 896 kip was calculated for E_{eq}, and 325.2 kip for G_{eq}.

An equivalent thickness of 0.536 in was calculated. The rim portion used a thickness of

0.36 in and the normal values for E and G.

5.3 Finite Element Analysis

A shell mesh (Figure 31) was partitioned into a rim portion and a center portion to

allow application of different material properties. Normal aluminum properties and the

actual thickness of the rim were assigned to the rim portion while the effective properties

and effective thickness were applied to the center portion. Because the deck panel was

mounted by fastening brackets along two edges and in order to be able to compare the

finite element results with experimental results, simply supported boundary conditions
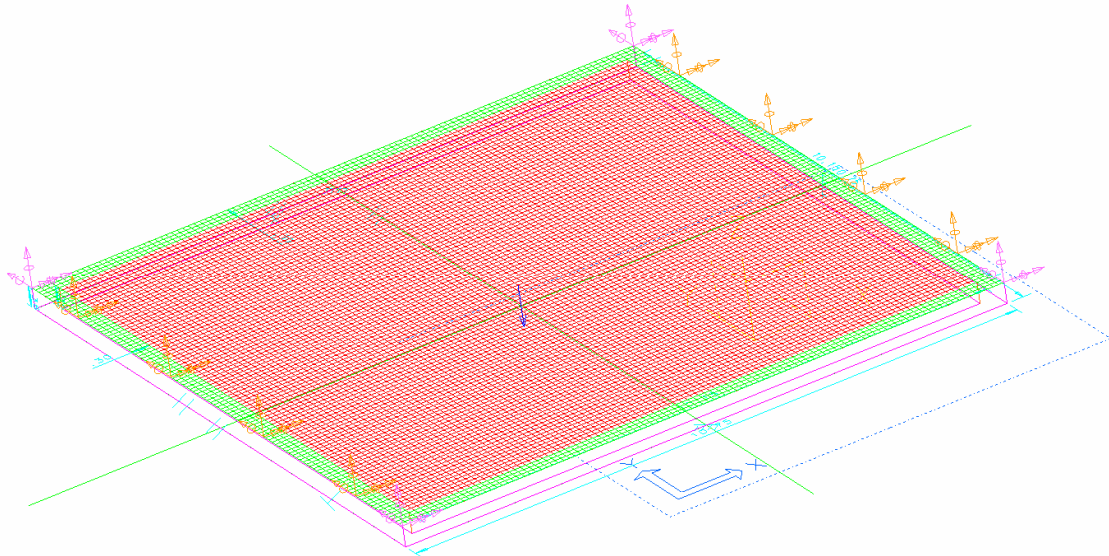
Figure 31. Finite element model with mesh, boundary conditions, and loading profile.

were applied to two opposing edges. A single point load was applied at the center of the plate.

The load was arbitrarily specified to be 300 lbf. The solution to the finite element model with the prescribed boundary conditions and loading is found in Figure 32. The corresponding stresses in the plate are found in Figure 33.

The results show what would have been expected. The simple support allowed two edges to rotate under the load. A gradient in the deflection results show the greatest deflection in the center of the panel. The stress results show how the rigid rim contains the greatest amount of stress.

To estimate the weight benefits of honeycomb compared to a solid panel, a finite element model was created similar to the previous model except the rim and center portions were given the same material properties and thickness. The thickness was then
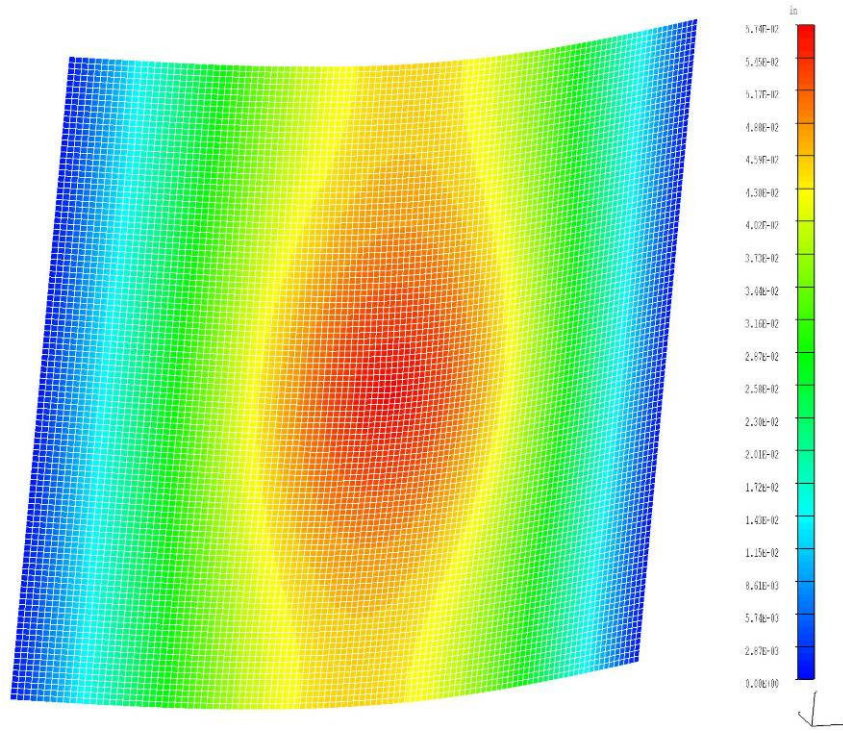
Figure 32. Solution to the FE model with a 300 lbf load (displacement results).
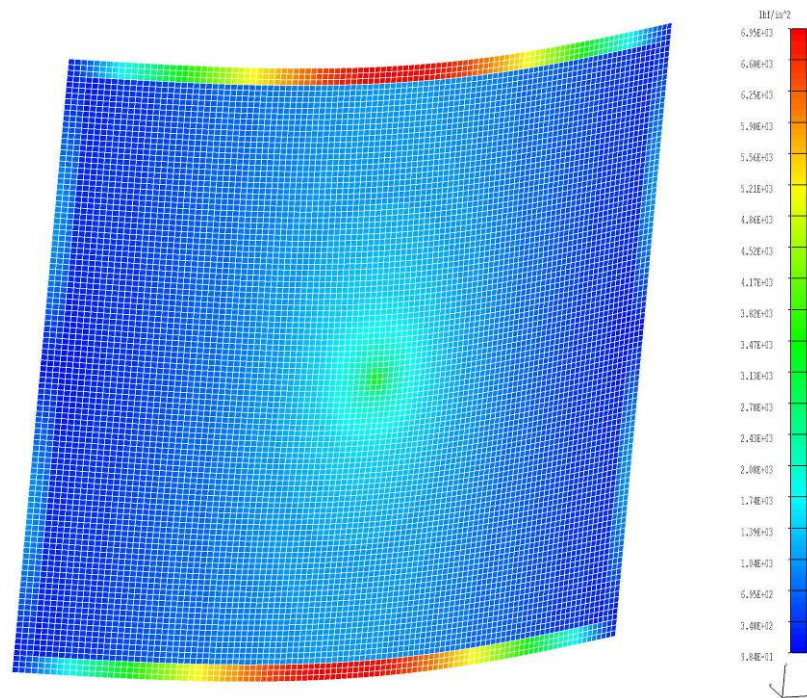
Figure 33. Solution to the FE model with 300 lbf load (stress results).

adjusted until the maximum deflection matched that of the effective panel under the 300 lbf load. The results are shown in Figure 34. The thickness to get such a deflection was 0.245 inches. The mass of such a plate would have been 2.79 pounds. This is a 55.6 percent increase in mass from the 1.794 pound deck panel.

The design criterion for such an aerospace structure is typically to design for a 20 G load with a safety factor of at least 2.4 against yielding. The results show a maximum Von Mises stress of 6,950 psi. The 3003 -H18 alloy of aluminum can withstand up to 27,000 psi before yielding. Thus the safety factor is 3.88 for a static load of 300 lbf. This exceeds the requirement of 2.4. Note that the maximum stress occurs at the center of the rim portion. The analysis has proven that some weight could be eliminated in the rim region.
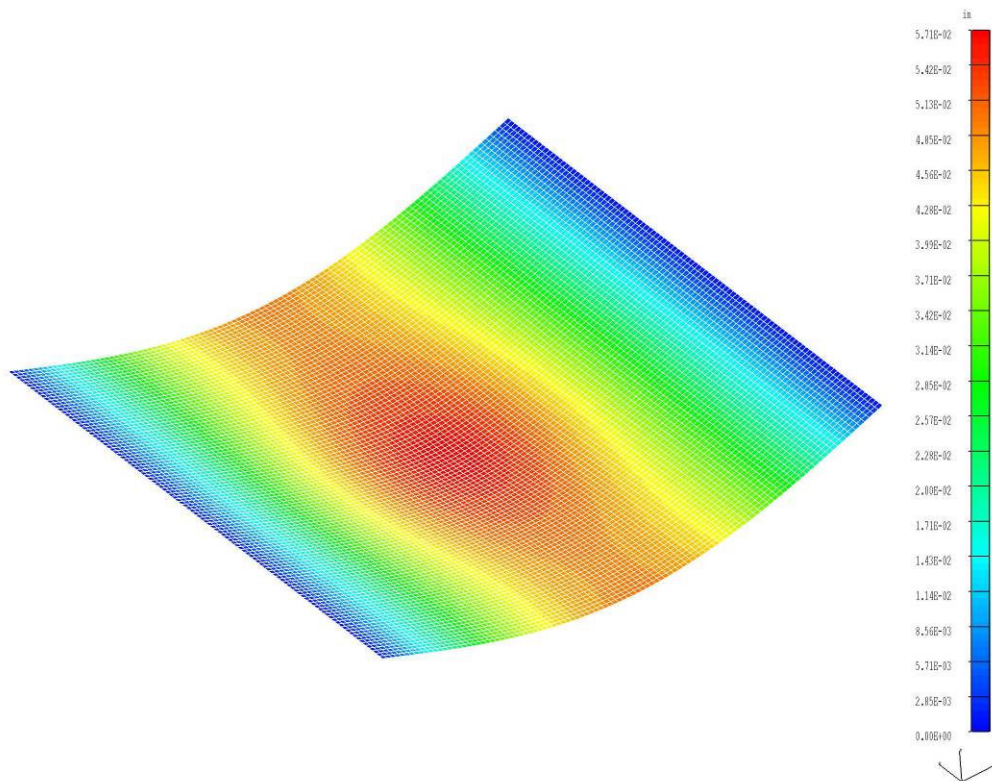
Figure 34. Solution to FE model with 0.245-inch thick plate.

CHAPTER 6

BUILD PROCEDURE DEVELOPMENT

6.1 Fabrication

Though development of the geometry of the deck panel is important, the manner in which it is fabricated is equally as important. There are many processes involved in creating the deck which if not performed in a specific sequence can cause tremendous problems. The build procedure was developed by creating a prototype of the deck panel. Following is the sequence of steps to fabricate the prototype panel.

First, a full solid model of the deck was created including all holes for the bolt pattern and mounting points, hollow core portions, and channels for embedding wiring. The solid model was then copied to make four separate files which were modified individually. Images of the four solid models are found in Figure 35.

The first model was a solid plate used to build up the bulk of the deck. Midway through the model was a channel groove that could have been used to embed wiring and a temperature sensor. The dimensions of the first model had the same length and width as the solid model of the deck. Its thickness was equivalent to the desired thickness composed of ultrasonically bonded material. The second model contained the

Figure 35. a) Solid model used for building up material and milling channels, b) Solid model used for milling honeycomb, c) Solid model used for adding top facing, d) Solid model for cutting bolt pattern.

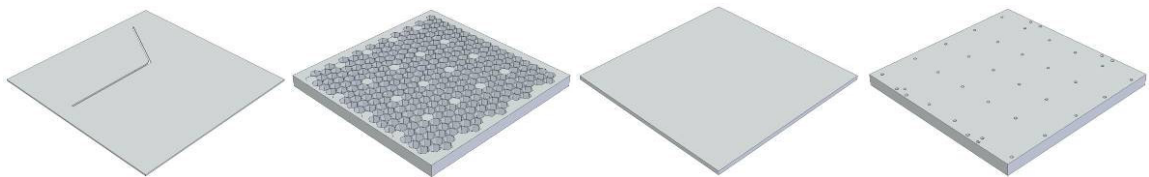milled honeycomb lattice with the reinforced rim and bolt pattern in tact. Its thickness was equivalent to the desired core thickness. The third model contained a solid plate that would be used as the skin on the core. Its thickness was equal to the desired skin thickness. The fourth solid model contained the holes for the bolt pattern and the bracket mounting points. Its thickness was equivalent to the entire thickness of the deck panel.

Next, Solidica's proprietary software, RPCAM, was used to generate the G-code for the toolpaths and tape lays for each model. A configuration file in the software enabled the user to modify the weld speed, amplitude of oscillation, and force for each model. The trim toolpaths for the perimeter of the second model were deleted as well as the bottom four trim toolpaths for the perimeter of the fourth model. This is because the deck is not ready to be removed from the baseplate until the final operation.

The next process in fabricating the deck was to prepare the Solidica machine for machining and UC. An ultrasonic couplant was applied to one face of the aluminum baseplate. This couplant enhanced thermal conduction between the heated platen and the aluminum baseplate while mitigating differential motion, due to ultrasonic vibration, between the two surfaces. The plate was then bolted to a heated platen located in the Solidica machine. A flatpass operation was used to clean the surface of the plate and to zero the plate with respect to the machine as shown in Figure 36 a.

The files for the first model were uploaded into the controller for the Solidica machine and the process was initiated. The machine tacked down 13 columns of tapes by using the sonotrode to spot weld the beginning and end of the tape along with a loose weld in between. This tack procedure allowed the tapes to be placed into the proper position so when the full amplitude was used to ultrasonically consolidate them to the
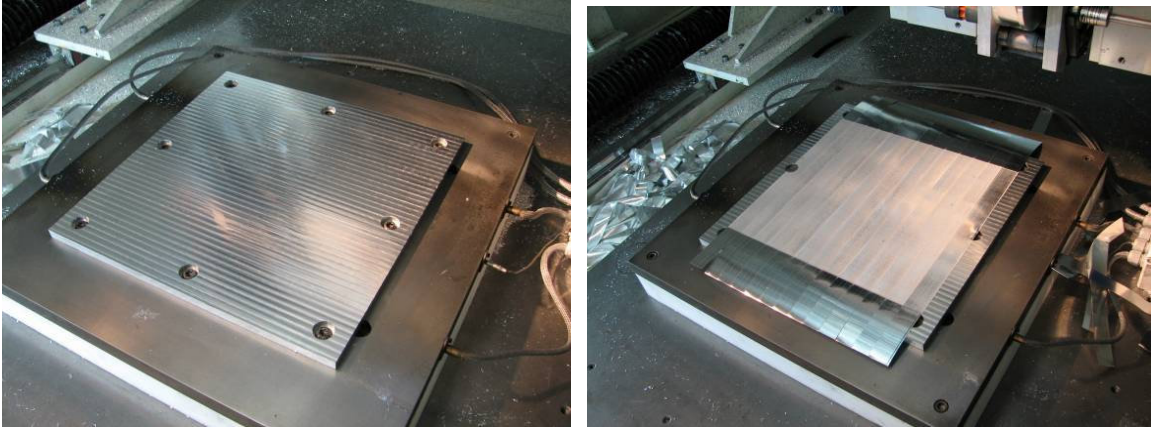
Figure 36. a) Clean baseplate, b) First layer of consolidated aluminum tapes.

baseplate, the tapes would not vibrate excessively enough to loose their proper position.

The tacked tapes were then consolidated by using the full force and amplitude and the

process was repeated for a second layer and so on as shown in Figure 36 b. Every four

layers, the machine used a cutting tool to automatically trim the excess tape length.

About halfway through the build, at 0.18 in of height, the machine automatically used a

0.125 in tool and machined the groove 0.14 in wide for the wiring and sensor. The

machine then continued to build until the thickness of the CAD model was attained.

After the build was finished, the files for the second CAD model were uploaded

into the Solidica machine. The vertical height of the build was changed in order to

correlate the Z heights for the milling operations. The program was initiated and the

machine milled out the honeycomb core as shown in Figure 37 a.

A close-up of the channel through the honeycomb is shown in Figure 37 b shows

how wiring for heaters, thermocouples, and other sensors can be embedded in the

structure. The height of the channel can be specified such that it passes thought the

centroid of the lattice, thus minimizing any damaging effect on the structural integrity.

Next, the files for the third model were uploaded into the machine and the Z

Figure 37. a) Milled substrate, b) Close-up of embedded channel.

height was set to be zero at the top of the fabricated build. After a final flatpass was

performed to clean the top of the honeycomb lattice and verify flatness, the program was

used to lay the skin on top of the core. Four layers of tapes were consolidated to the

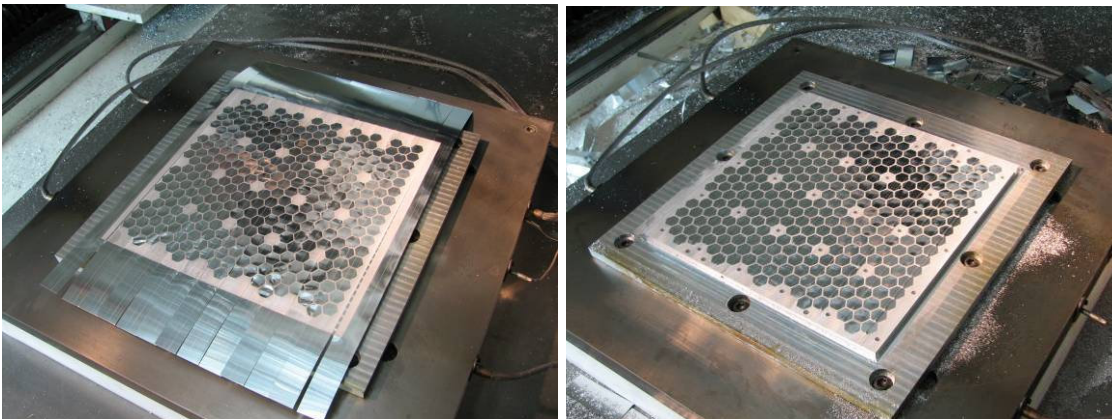surface (Figure 38 a) and the tapes were offset each layer to avoid the creation of a

parting line.

Figure 38. a) Fist layer of top facing consolidated on honeycomb core, b) Prototype deck
panel with bolt pattern milled out.

Next, the files for the fourth model were uploaded and the process was initiated. The machine proceeded to drill the holes for the bolt pattern as well as the holes for the mounting brackets. In the prototype deck, the trim toolpath around the perimeter of the deck was actually made smaller than the perimeter that was fabricated using the other files. This was done to remove any edge effects that could cause nonoptimal bonds in the part. Trimming away the weak portion revealed a new clean surface that would serve as the final dimensions of the deck. The trimmed deck is shown in Figure 38b.

Next, the unusable portion of the aluminum plate was removed by turning the plate over and milling the back down until the desired skin thickness remained on the deck panel as shown in Figure 39 a. This operation also enabled a flat surface to be created that would be used as the mounting surface for the payload which would be attached to the panel.

Next, the deck was removed from the Solidica machine and cleaned up using a band saw and manual mill as shown in Figure 39 b. The manual segment of the procedure was trivial and only necessary to clean up edges which were connecting the deck panel to the aluminum baseplate. A final operation involved threading the mounting points and installing helicoils for added strength. The resulting deck panel is shown in Figure 40.
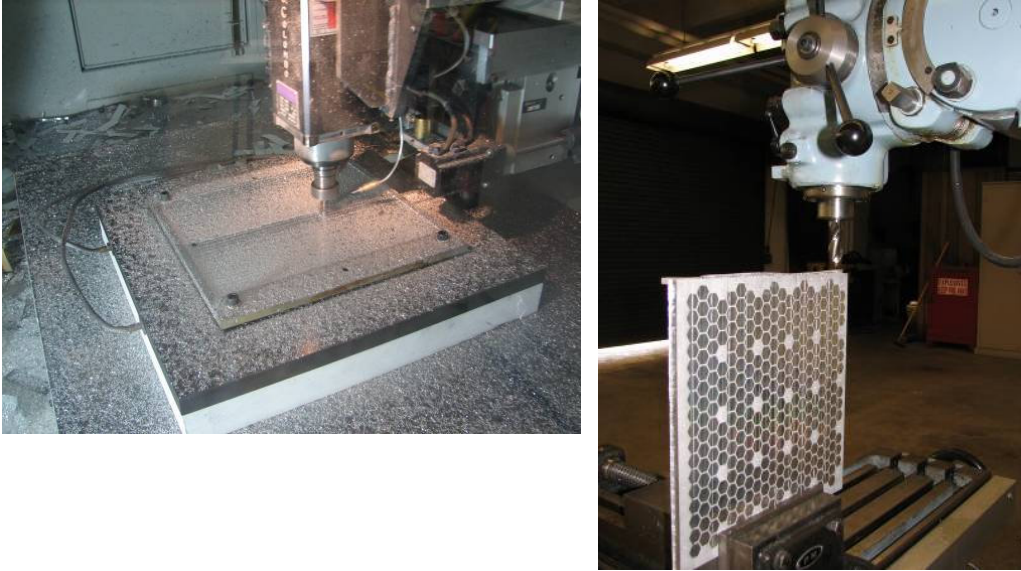
Figure 39. a) CNC mill removing excess material from baseplate, b) Final operation to remove segment of baseplate.
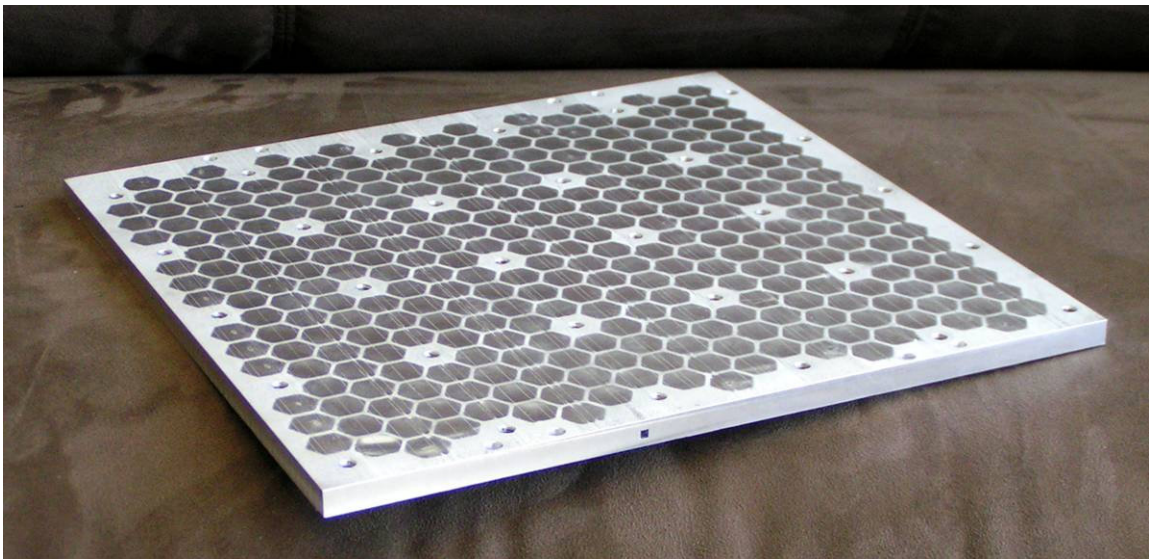
Figure 40. Finished prototype deck panel.

CHAPTER 7

STRUCTURAL TESTING

7.1 Three-Point Bend Testing

With the prototype deck fabricated, it was possible to test the panel for

comparison with the finite element results. As was discussed in the literature survey, 3-

point bending (Figure 41) could be used to determine the ratio of deflection to loading to

give the stiffness for the assembled core and facings.
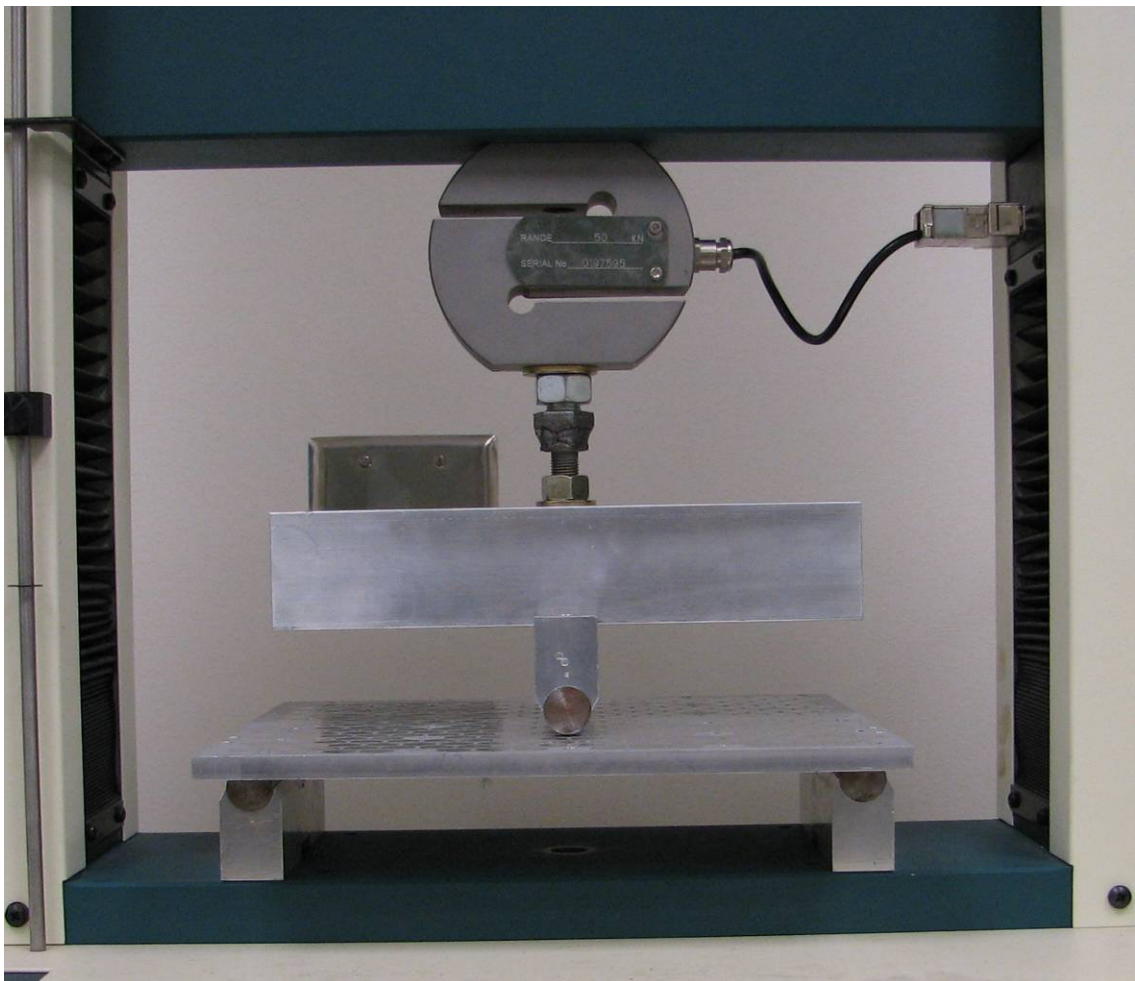
Figure 41. Three-point bend testing apparatus with prototype deck panel installed.

The load cell used was a Tinius Olsen load cell with an 11250 lbf capacity. It had the capability of measuring a force to within ± 0.5 percent of the indicated load when operating within the range which was tested. The extension was accurate to within ±0.0004 inches.

The 3-point bend test was performed by placing the prototype panel on two supported cylinders as shown in Figure 41. The cylinders created a simply supported line support in the same location it was applied in the finite element model. A third supported cylinder was attached to the load cell and brought down very close to the panel. The force and extension were referenced at zero and then the machine was programmed to lower at a rate of 0.01 in/min. The resulting data can be found in Figure 42.

The plot shows a nonlinear stiffness for the first 0.03 inches and then a linear trend for the remainder of the test. The nonlinear portion was due to the fact that the apparatus was not touching the deck when the experiment was initiated. Some minor adjustments in the deck and fixture resulted in the nonlinear trend. The linear region showed a stiffness of 8630 lbf/in.

For comparison with the finite element model, the deflection at 300 lbf was noted. The correct deflection was obtained by noting when the force measurements began in the recorded data and using that as the reference for zero deflection. The experimental data showed a deflection of 0.0506 inches. This was compared with the finite element results of 0.0574 inches. This gave a percent difference of 11.85 percent. The deflection at 200 lbf for the 3 point bend test was 0.0389 inches. This was compared with the finite element deflection of 0.0383 inches for the same force. This data point corresponded
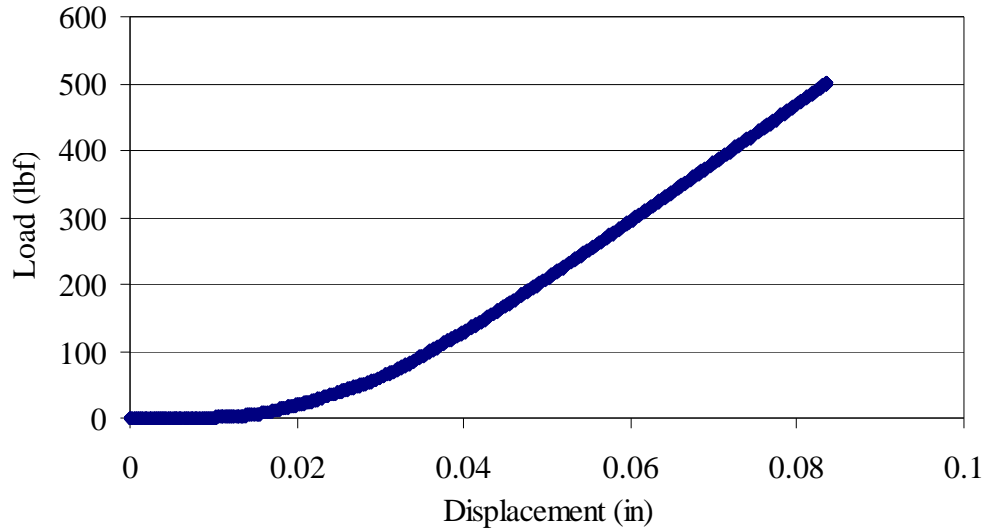
Figure 42. Stiffness of prototype deck panel from 3-point bend test.

even closer, having only a 1.57 percent difference between the experimental and

numerical results.

The difference was most likely due to assumptions made in the equivalent skin

method for the finite element model as well as discrepancies between the setup of the

model and the setup of the 3-point bend test. There was also some error due to the fact

that at a load around 300 lbf, the resolution of the load cell was 1.5 lbf. For the purposes

of showing a general trend between experimental and numerical results, the results were

sufficient. The stress results given in the finite element model could be considered

sufficiently accurate given the application of a small safety factor.

7.2 Vibration Testing

The prototype panel was tested on a vibration table at the Space Dynamics

Laboratory in Logan, Utah. A sine sweep test was performed in order to find the

resonant frequencies and to verify robustness in the design. The setup of the vibration

table, the mounting fixture, and the prototype deck are shown in the Figure 43.

The results from the sine sweep at .25 G's are shown in Figure 44. The deck was found

to have a first natural frequency of 560 Hz. The deck was also tested at 1 G and 0.5 G's

and found to have first natural frequencies of 553 and 559 Hz, respectively. This shift in

frequencies indicates variance in damping for different loads and implies the deck has a
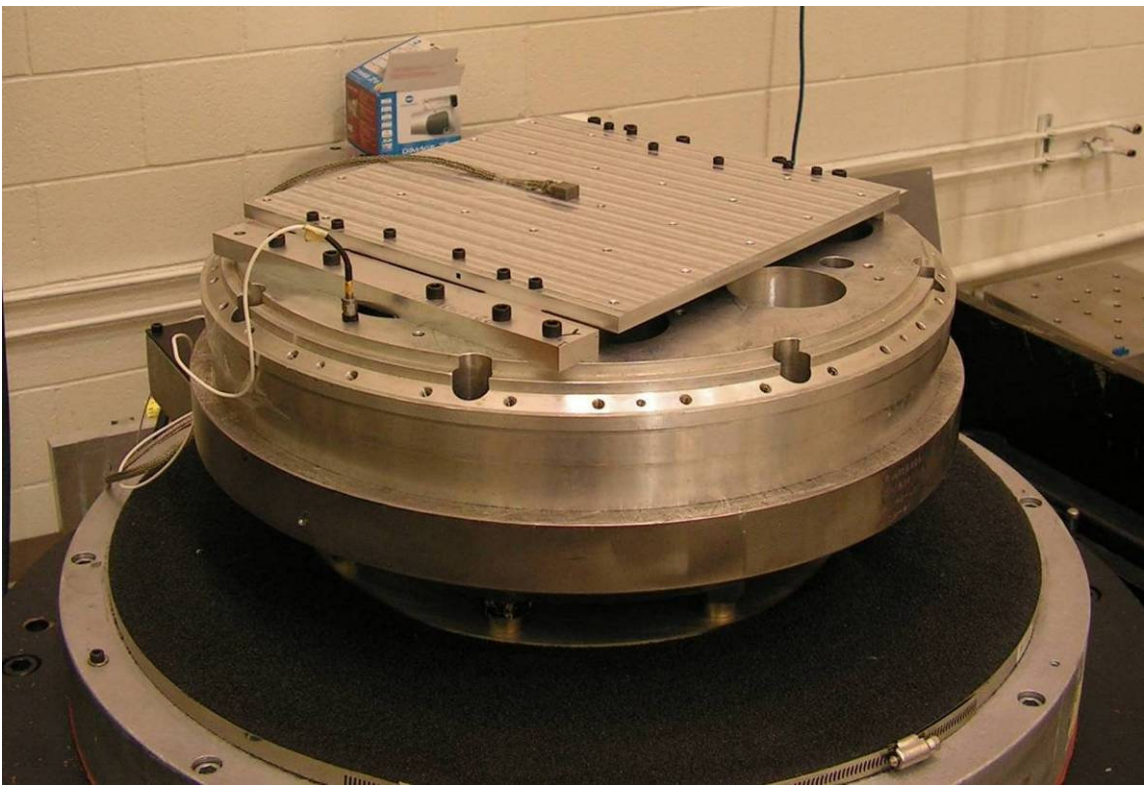
nonlinear response.

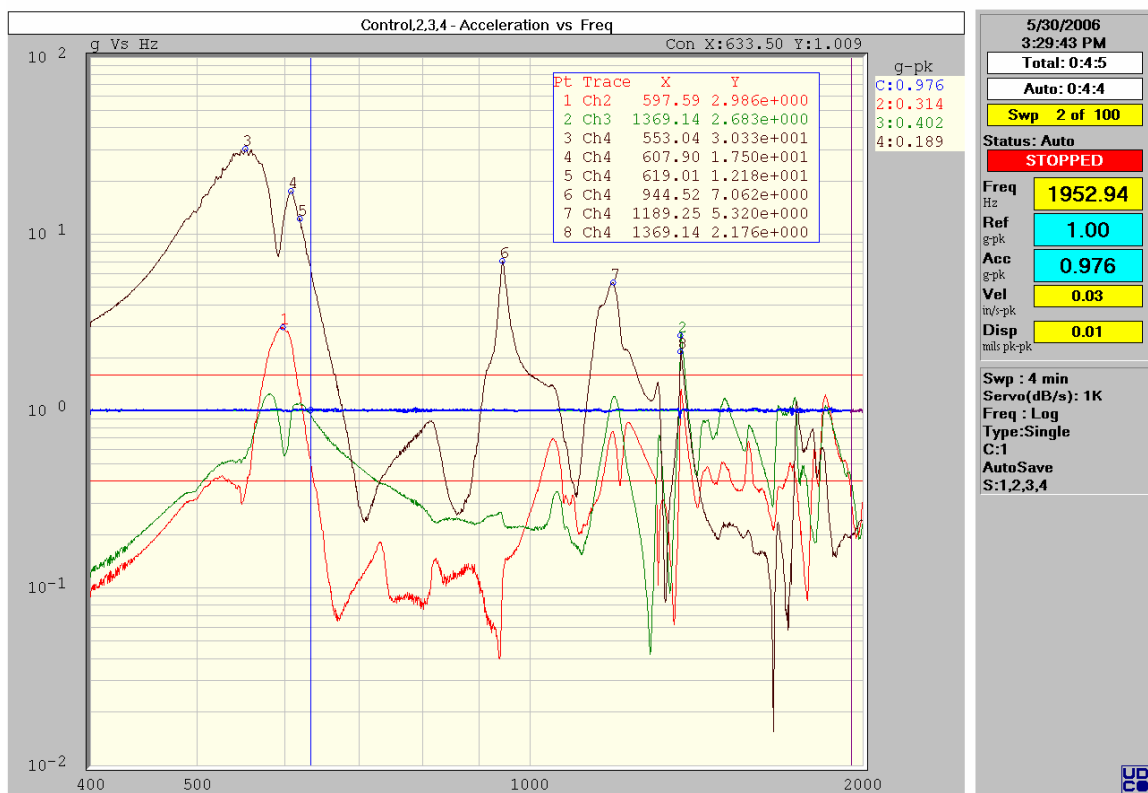Figure 43. Vibe test setup with prototype deck installed with accelerometer installed.

Figure 44. Vibration test results for sine sweep from 0 to 2000 Hz.

CHAPTER 8

CASE STUDY: TOROID

As a final demonstration of the capabilities of UC in fabrication of a deck panel, a final deck panel was fabricated for the TOROID spacecraft. This deck panel used the geometry designed for the integrative CAD model and the testing results of the prototype deck panel to create a structure that was better fit for spaceflight and customized for the small satellite at Utah State University.

8.1 TOROID Project Overview

Utah State University is currently participating in the 4th University Nanosatellite Competition directed by the Air Force Research Laboratory (AFRL). The purpose of this competition is to develop the small satellite technology area while providing workforce training for university students. It is sponsored by the American Institute for Aeronautics and Astronautics (AIAA) and supported by both the National Aeronautics and Space Administration (NASA) and the Air Force Office of Scientific Research (AFOSR).

Utah State University's entry into the competition is the Tomographic Remote Observer of Ionospheric Disturbances (TOROID). TOROID will demonstrate both scientific and technological capabilities as the satellite is fabricated, tested, and eventually put into orbit around the earth. The scientific mission of TOROID is to observe scintillations in the low latitude ionosphere with increased fidelity. The data will provide the scientific and military communities with a greater understanding of the morphology and equatorial phenomena which currently impede accurate space based geolocation.

There were several reasons a deck was needed in the structural design of the bus. First of all, the Utah State University Satellite (USUSat) design emphasized the importance of modularity by using panels. Components for the various subsystems were attached to the panels which were, in turn, assembled into a boxlike structure. This also allowed each panel to be tested individually for vibration and thermal effects. There was very little space for mounting a new payload such as the TOROID science instrument. The problem is that the science instrument required a large area and cantilevered support (Figure 45). While the inside of the panels of the boxlike structure was covered with components and harnessing, the majority of the interior volume of the satellite was empty. This empty space, however, was the perfect place to install a horizontal deck panel, upon which the science instrument could be mounted. It was decided to use UC on this deck which would become part of the current TOROID structure. As the deck employed new fabrication techniques and multifunctional capability, its development comprised one of the technological objectives of the TOROID mission.
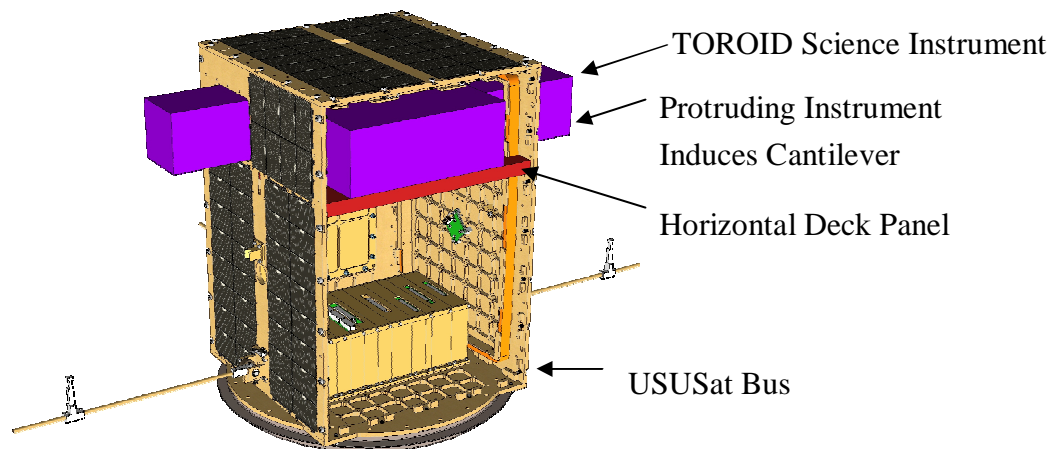
Figure 45. TOROID spacecraft with simplified science instrument.

8.2 Modifications for the Final Deck Panel

The overall dimensions of the final deck panel were governed by the footprint in the TOROID spacecraft. As shown in Figure 46, the maximum thickness of the panel was limited to 0.5 inches. This dimension was limited by the battery box below the deck and the release mechanism above the deck. The length and width of the deck were also decreased due to the flanges of the torquer coils and the battery box shown in Figure 46. Caution was taken to avoid problems with harnessing and the battery box.

One major focus of USUSat has been a modular design with a standard bolt pattern. This pattern is currently part of the design of the side panels. They contain an orthogrid with reinforced tapped holes every 1.275 inches. The prototype deck panel contained a bolt pattern but it was coincident with the honeycomb pattern. For the final deck panel, the bolt pattern was treated independently of the honeycomb. Reinforced cylinders were input into the CAD model to allow holes to be machined and tapped.
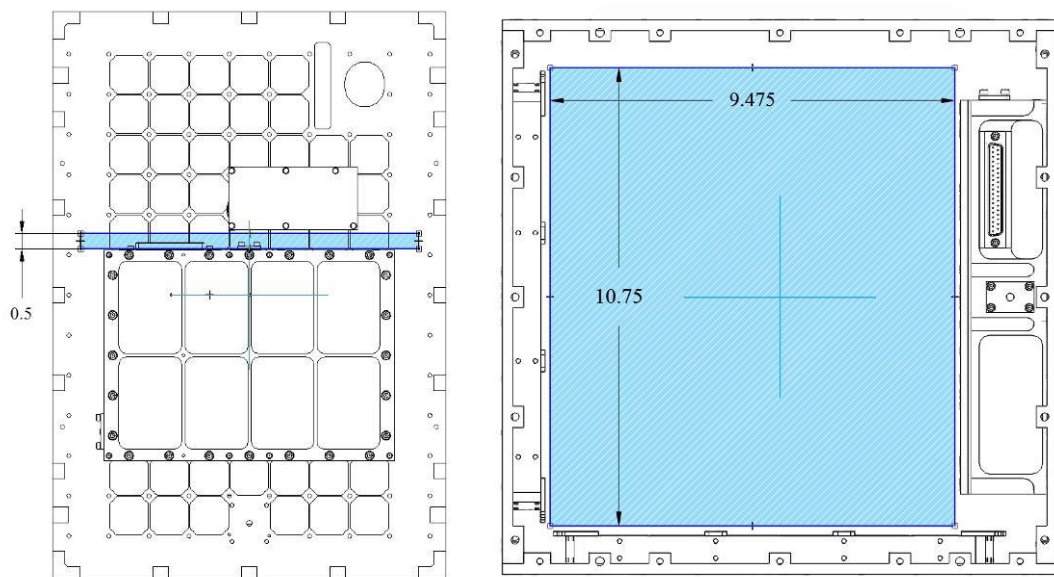
Figure 46. Footprint of space for final deck panel (side and top views).

This method of creating a bolt pattern reduced the amount of material in the panel and thus increased its efficiency. The pattern was also aligned such that the fastening points that would be used to fasten the deck to the satellite were attached to the rim of the deck for added support. These fastening points were aligned on an edge perpendicular to the direction of the tapes. This was done so that when the deck panel is loaded, it will not be stressing the tapes in their side-by-side interface.

The rim around the perimeter of the deck panel acts as a stiffener in the satellite. This will help maintain the rigidity in the in-plane axis. From the finite element results, the rim on the prototype deck was found to be excessively thick so the rim was reduced to a simple rectangular beam of 0.25 inches in width. The final CAD model of the TOROID deck panel without its top facing is found in Figure 47. The structural drawing package is found in Appendix A.
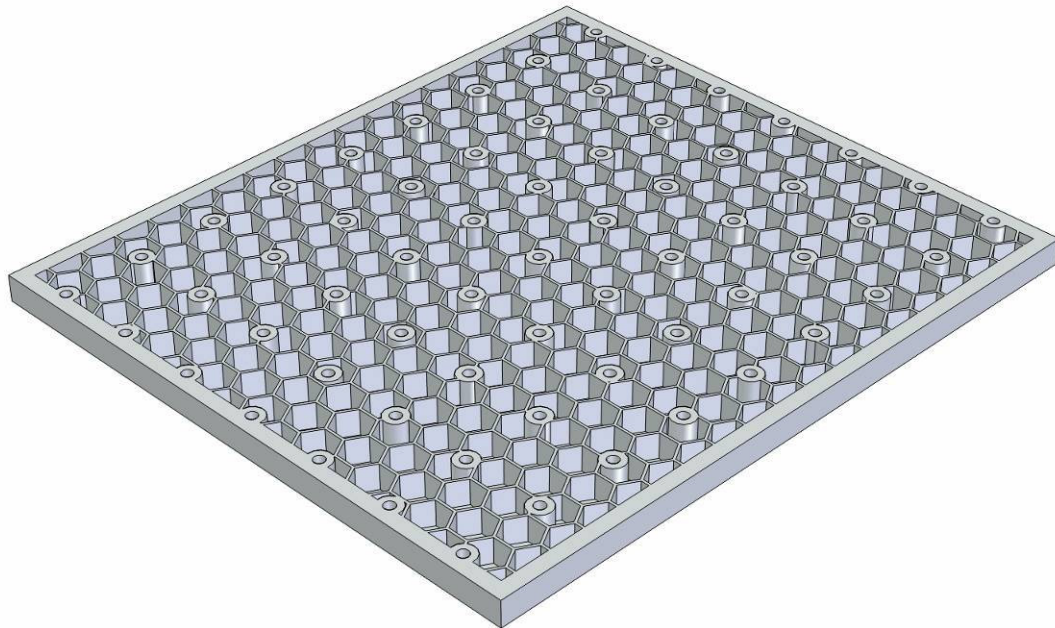
Figure 47. CAD of final deck panel.

Small holes were used to perforate the honeycomb sections. This was done since completely enclosed cavities have a tendency to rupture in space due to the decreased pressure in the space environment. This could have also been accomplished by milling a tiny channel through the centroid of the honeycomb cell walls as well.

The final deck panel did not contain any enclosed channels such as the one milled in the prototype deck panel. This is because the mission requirements of TOROID did not necessitate any such channel. The prototype deck panel contained the channel as a proof of concept, that objects such as sensors and wiring can be embedded in the structure.
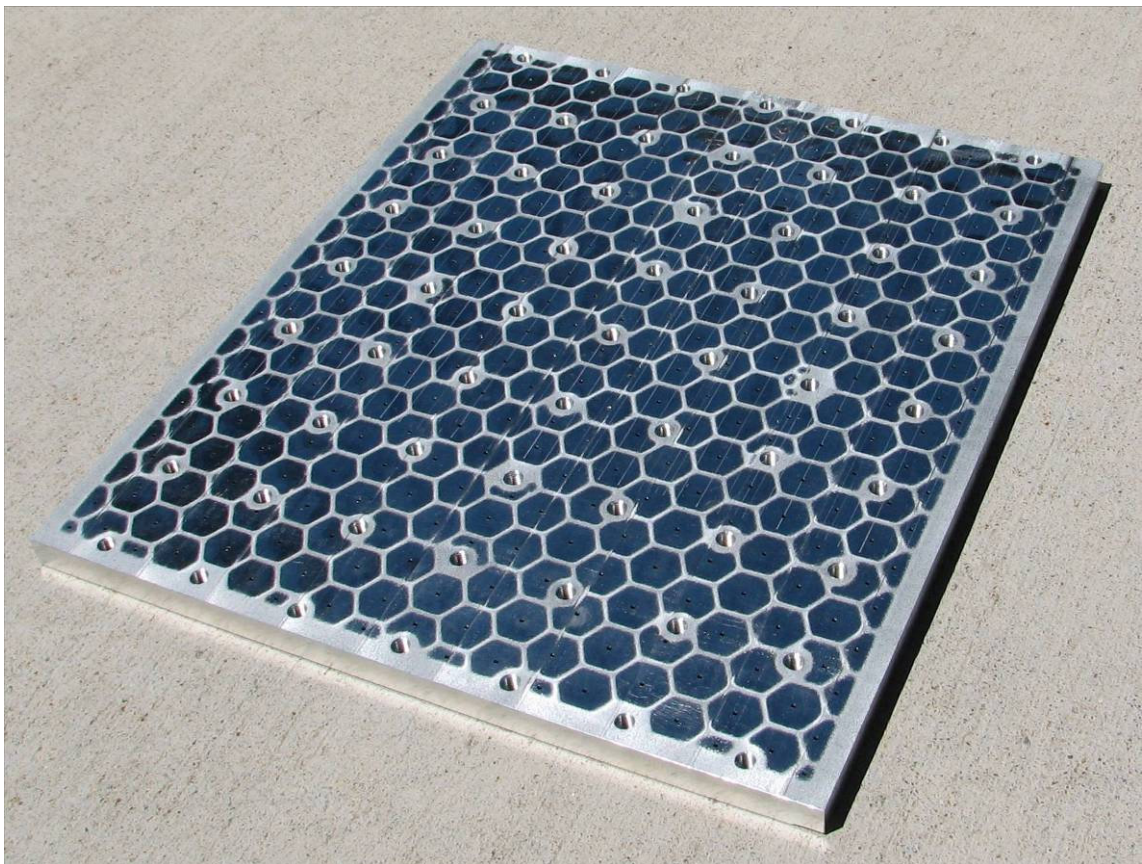
Figure 48. Photograph of completed final deck panel.

The final deck panel was fabricated (Figure 48) using the same procedure as that developed for the prototype deck panel. The TOROID deck panel is much lighter, at 1.38 lb compared to the 1.79 lb prototype deck. The overall dimensions of the final product are 10.73 x 9.45 x 0.42 inches. The honeycomb core was composed of regular hexagons 0.31 inches in diameter and 0.372 inches tall. The same web thickness of .040 inches was used. The facings were 0.024 inches thick on both faces. Nonlocking 8-32 helicoils were inserted into the threaded bolt pattern in the deck. These were to provide resistance against wear.

8.3 Economy of Using UC for Deck Plate Fabrication

The costs involved in fabricating the TOROID deck are found in Table 1. The table has the material costs and labor costs separated. Note that the labor costs were approximated by multiplying the time to complete each task by $38. The italicized numbers indicate that a 50 percent reduction in cost was applied. This was done because such processes could be left unattended on the machine. The total time for the build was about 56 hours. Because about 16 hours were during the night, the deck was completed during a full work week of 40 hours. The majority of time was in machining the honeycomb grid and bolt pattern. These tasks consumed a tremendous amount of time due to the inefficiency of the milling machine used in our specific UC machine. Because the machine was not made for heavy machining, it possesses a small spindle which can not remove material at a very fast rate. The bolt pattern also took considerable time due to excessive lengths for toolpaths. Both of these operations could be greatly enhanced as far as speed is concerned by performing them in a CNC with a more powerful spindle.

Table 1. Cost of Fabricating TOROID Deck

Materials	Time (hours)	Cost
Aluminum 3003 tape	-	25.59
Isopropyl alcohol	-	79.35
Aluminum 3003 plate	-	100.23
End mills	-	24.40
Helicoils	-	13.23
Wear on helicoil tap, tapping fluid, ultrasonic couplant, gloves, rags	-	15.00
Total materials	-	**257.80**
Labor		
Setup machine	0.50	19.00
Plate find/Plate clear/Upload program	0.50	19.00
Clad bulk material w/ trim	8.00	*152.00*
Machine honeycomb grid	24.00	*456.00*
Machine bolt pattern	8.00	*152.00*
Flat pass	0.50	19.00
Place facesheet on honeycomb	1.00	38.00
Trim to correct dimensions	1.50	57.00
Machine vent holes	2.00	*38.00*
Setup for removing base plate	0.50	19.00
Mill off baseplate	3.25	123.50
Clean edges and deburr	1.50	57.00
Tap and insert helicoils	2.00	76.00
Adaptation for changes	3.00	114.00
Total time	**56.25**	**1,339.50**

The total cost of the build was $1,597.30. This cost is comparable to the cost to machine one of the panels on the USUSat bus. An informal estimate was done by a commercial small satellite producer. They found that a similar panel fabricated out of composites would cost $2,200 to $3,200. Material costs would have been similar but labor costs would have greatly surpassed those for fabricating the TOROID deck. This identifies out one of the main advantages of the UC built panel over a traditionally fabricated panel. Traditional methods require the use of composites which are incredibly labor intensive since the composite lay up involves precise assembly and curing in an oven.

The mass was estimated for an equivalent composite panel with potted inserts to be 0.485 lb. This identifies one of the disadvantages of UC. Because of the incredible properties of composite materials, such as carbon fiber reinforced polymers, a tremendous amount of mass can be saved by using very little material. In small satellites such as USUSat, though, this has very little impact. The satellite is already very small and light. The UC built deck also has the added benefit in that it can very easily be made into a multifunctional structure.

CHAPTER 9

CONCLUSIONS AND FUTURE WORK

Conclusions

Using UC in conjunction with a CNC mill has opened up a new fabrication technique which allows satellite structures to be built with the benefits of additive manufacturing. Many of the typical problems found in additive manufacturing can be avoided due to the full metallurgical bond, low operating temperatures, and low cost associated with UC. Because the structure can be built up layer by layer, internal features such as ribs, voids, and various components such as thermal sensors and wiring can be embedded into a structure. The work done for this thesis has identified the configurations which allow such structures to be created.

This fabrication method enabled the creation of a lightweight and stiff panel similar to a honeycomb sandwich panel but without fabrication issues involving epoxy and inserts. The UC process becomes a particularly useful fabrication technique since the facings of the sandwich panel can be consolidated to a lightweight honeycomb core. The amount of complexity for assembly of this type of sandwich panel is much less than for traditional methods.

With a solid model of the deck, and a procedure for fabricating the deck, a deck can currently be produced in about a week. Experimental results correlate well with finite element results using equivalent skin methods.

The results of this thesis have proven that it is possible to make a structure that competes with structures found in industry today. In order to become a disruptive technology, such as the transistor in the computer world, future work must be done to

make UC the fastest, cheapest, and most robust fabrication technique for producing satellite hardware.

Future Work

There is a plethora of work that can be performed in the future to improve the quality of structural panels that can be produced using UC. The most significant of these is the implementation of a support material apparatus in the Solidica machine. The support material would allow each layer of the facing to bond fully to the layer below it. Currently, bonding is only achieved directly over the honeycomb cell walls. This would also reduce any dimpling in the facing.

The facings would also benefit tremendously by using fiber reinforcement. There is currently a pre-impregnated tape that contains filaments of aluminum oxide. Integration of this type of tape into the facing would make the sandwich panel much stronger. Also, the mass of the panel could be dramatically reduced by using a stronger material such as the 6061 aluminum alloy. In addition, 6061 is more accepted in the aerospace community due to its extensive use in successful missions.

The time it takes to produce a deck panel could be cut down from one week to approximately one day with the use of a more powerful mill, more machinable alloys, and with modifications to the toolpaths generated by Solidica's proprietary software. Often times, the toolpaths are greatly excessive in travel distance. The motion of the machine when laying tapes could also be tightened to prevent excessive travel.

The final deck panel still lacks testing with the final payload used for TOROID. As the payload hardware is fabricated and testing of the entire TOROID spacecraft begins, valuable information about the deck panel when put under dynamic loading will

be investigated.

      The final area that can be completed in the future is the integration of other subsystems into the deck panel. Items such as heat pipes, antennas, wiring, thermocouples, low profile heaters, embedded computers, connectors, and printable batteries will eventually be integrated into the design and may perhaps someday be automated similar to the process of printing a printed circuit board in the electronics world.

REFERENCES

Allen, H.G. 1969. *Analysis and design of structural sandwich panels*. London, UK: Pergamon Press Ltd.

Ashby, B.J. 2001. *USUSat structure and design analysis*. Masters thesis, Utah State University.

ASTM. 2004. *Standard test method for floating roller peel resistance of adhesives*. ASTM D 3167-03a (2004). West Conshohocken, PA: ASTM International.

Bitzer, T. 1997. *Honeycomb technology: materials, design, manufacturing, applications and testing.* London, UK: Chapman & Hall.

Chua, C.K., K.F. Leong, and C.S. Lim. 2003. *Rapid prototyping: principles and applications*. 2nd ed. Singapore: World Scientific Publishing Co.

Cook, R.D., D.S. Malkus, and M.E. Plesha. 1989. *Concepts and applications of finite element analysis*. 3rd ed. New York: John Wiley and Sons.

Daniels, H.P.C. 1965. Ultrasonic welding. *Ultrasonics*. October-December Issue, 190.

DiPalma, J., J. Preble, M. Schoenoff, and S. Motoyama. 2004. *Applications of multifunctional structures to small spacecraft.* 18th Annual AIAA/USU Conference on Small Satellites. Logan, UT.

Dewhurst, P. 2005. A general optimality criterion for strength and stiffness of dual-material-property structures. *International Journal of Mechanical Sciences* 47, no. 2:293-302.

Gao, Y. 1999. *Mechanical analysis of ultrasonic metal welding for rapid prototyping*. Masters thesis. Tufts University.

Gibson, M.F., and M.F. Ashby. 1988. *Cellular solids: Structure and properties*. Elmsford, New York: Pergamon Press.

Grediac, M. 1993. A finite element study of the transverse shear in honeycomb cores. *International. Journal of Solids and Structures* 3, no.13:1777-88.

Hexcel. 1999. *Hexweb honeycomb attributes and properties*. Pleasanton, CA: Hexcel.

Janaki Ram, G.D., Y. Yang, J. George, and C. Robinson, eds. 2006. *Improving linear weld density in ultrasonically consolidated parts*. 17th Solid Freeform Fabrication Symposium.

Johnson, N. 1998. *Rapid prototyping using ultrasonic metal welding*. Masters thesis, Tufts University.

Kingston, J. 2005. *Modular architecture and product platform concepts applied to multipurpose small spacecraft*. 19th AIAA/USU Conference on Small Satellites, Logan, UT.

Kong, C. 2005. *Investigation of ultrasonic consolidation for embedding active/ passive fibres in aluminium matrices*. Ph.D. Thesis, Loughborough University.

Kong, C., R.C. Soar, and P.M. Dickens. 2004. Optimum process parameters for ultrasonic consolidation of 3003 aluminium. *Journal of Materials Processing Technology* 146 no. 2:181-187.

Kong, C., R.C. Soar, and P.M. Dickens. 2003. Characterization of aluminium alloy 6061 for the ultrasonic consolidation process. *Materials Science and Engineering*: Part A 363, no. 1-2: 99-106.

Larson, W. J. 2003. *Spacecraft structures and mechanisms: From concept to launch*. El Segundo, California: Microcosm, Inc.

Lewin, A.W. 2004. *Evaluating the present and potential future impact of small satellites. 18th Annual AIAA/USU Conference on Small Satellites*, Logan, UT.

Matsuoka, S. 1998. Ultrasonic welding of ceramics/metals using inserts. *Journal of Materials Processing Technology* 75:259-265.

Mosher, T., and B. Stucker. 2004. *Responsive space requires responsive manufacturing*. 2nd Responsive Space Conference, Los Angeles, CA.

NASA (National Aeronautics and Space Administration). 1992. *Guidelines for the selection of metallic materials for stress corrosion cracking resistance in sodium chloride environments*. NASA Technical Standard, MSFC-STD-3029.

Osgood, C. 1966. *Spacecraft structures*. Englewood Cliffs, NJ: Prentice Hall.

Quincieu, J. 2003. *USUsatII design and fabrication standards*. USUSat document # 1015031502, Rev. A.

Paik, J.K., A.K. Thayamballi, and G.S. Kim. 1999. "The strength characteristics of aluminium honeycomb sandwich panels," *Thin-Walled Structures* 35 no. 3:205-231.

Panetta, P.V., H. Culver, J. Gagosian, and M. Johnson, eds. 1998. *NASA-GSFC nanosatellite technology development*. Proceedings of the 12th AIAA/USU Conference on Small Satellites, Logan, UT.

Robinson, C.J. Zhang, G.D. Janaki Ram, and E.J. Siggard, eds. 2006. *Maximum height to width ratio of freestanding structures built using ultrasonic consolidation*. Solid Freeform Fabrication Symposium, Austin, TX.

Rodgers, L., N. Hoff, E. Jordan, and M. Heiman, eds. 2005. *A universal interface for modular spacecraft*. Proceedings of the 19th AIAA/USU Conference on Small Satellites, Logan, UT.

Sarafin, T. P. 1995. *Spacecraft structures and mechanisms: From concept to launch*. El Segundo, CA: Microcosm, Inc.

Shirgur, B., and D. Shannon. 2000. *The design and feasibility study of nanosatellite structures for current and future fsi micromissions*. AIAA Small Satellite Conference, 2000.

Triplett, M.H. 1995. *Static and dynamic finite element analysis of honeycomb sandwich structures*. Masters thesis, University of Alabama.

Tsujino, J., K. Hidai, A. Hasegawa, and R. Kanai, eds. 2002. Ultrasonic butt welding of aluminum, aluminum alloy and stainless steel plate specimens. *Ultrasonics* 40:371-374.

Vinson, J.R. 1999. *The behavior of sandwich structures of isotropic and composite materials*. Lancaster, PA: Technomic Publishing.

Weare, N.E., J.N. Antonevich, and R.E. Monroe. 1959. *Fundamental studies of ultrasonic welding*. AWS 40th Annual Meeting, Chicago, IL.

White, D. 2002. *Ultrasonic consolidation for direct metal fabrication*. SME conference, Cincinnati, USA. [CD-ROM].

APPENDICES

Appendix A

Structural Drawing Package

VIEW A-A

DETAIL B

Deck Panel
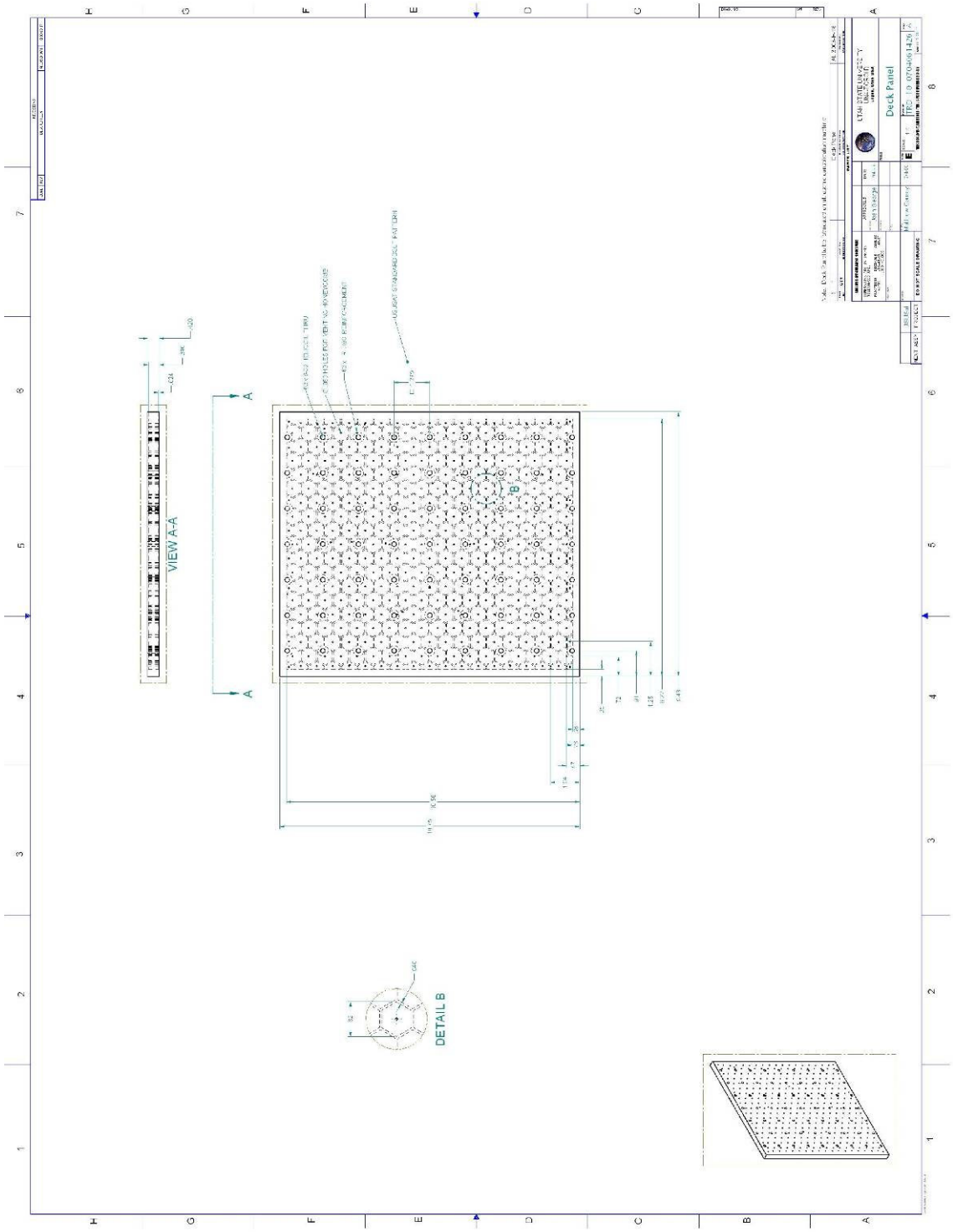
Appendix B

Permission to use copyrighted material

Emailed Request for Permission to use Figure 1

Request Email:

Dr. Soar,

I have come across an individual grant review report prepared by yourself and Choon Yen Kong. There is a very well prepared image illustrating the ultrasonic consolidation process. I have included the image you put in the report. I wish to ask for your permission to use this figure in my thesis entitled: Utilization of Ultrasonic Consolidation in Fabricating Satellite Decking. I am a Masters student and professional engineer working for Dr. Brent Stucker at Utah State University. If you give me permission to use the image, I will make sure to note in the caption who it came from. Please respond quickly. Thanks.

Josh George

Response:

Hi Josh

Thank-you for taking the time to contact me - please go ahead

Rupert

Dr Rupert Soar
The Rapid Manufacturing Research Group and Freeform Construction Laboratory

Wolfson School of Mechanical and Manufacturing Engineering
Loughborough University
Loughborough
Leicester
LE113TU
Tel: +44 (0) 1509 227637
Fax: +44 (0) 1509 227549
Cel: +44 (0) 7973219624
www.freeformconstruction.co.uk
www.sandkings.co.uk
www.lboro.ac.uk/departments/mm/research/rapid-manufacturing/people/Soar.html

Emailed Request for Permission to use Figure 6

Request Email:

Chris,

There is a segment in my thesis that discusses the problems of building ribs using UC. I would like to include the image for data you obtained on the height to width ratio for freestanding ribs in the following paper:

Robinson, C.J. Zhang, G.D. Janaki Ram, and E.J. Siggard, eds. 2006. Maximum height to width ratio of freestanding structures built using ultrasonic consolidation. Solid Freeform Fabrication Symposium, Austin, TX.

Will you grant me permission to include this image in my thesis. I will make sure to reference your work and the related figure. Thanks.

Josh George

Response:

You have my permission!